Blood pressure variability compromises vascular function in middle-aged mice.

Perenkita J. Mendiola[1], Philip O'Herron[1], Kun Xie. [1], Michael W. Brands[1], Weston Bush[1], Rachel E. Patterson[1], Valeria Di Stefano[1], Jessica A. Filosa[1].

Department of Physiology[1], Medical College of Georgia, Augusta University, Augusta, Georgia, USA

Running Title: *Blood pressure variability impairs neurovascular function*

Correspondence should be addressed to:
Jessica A. Filosa
Department of Physiology
Augusta University
Augusta, GA. 30912. USA
e-mail: jfilosa@augusta.edu
Telephone: 706-726-5336

Total words of the manuscript: 5486

Running headline (no more than 50 characters)

ABSTRACT

Blood pressure variability (BPV) has emerged as a significant risk factor for cognitive decline and dementia, independent of alterations in average blood pressure (BP). However, the impact of large BP fluctuations on neurovascular function remains poorly understood. In this study, we developed a novel murine model of BPV in middle-aged mice using intermittent Angiotensin II infusions. Radio telemetry confirmed that 24-hr BP averages in BPV mice remained comparable to controls, demonstrating BPV in the absence of hypertension. Chronic (20-25 days) BPV resulted in a blunted bradycardic response and cognitive deficits. Two-photon imaging revealed heightened pressure-evoked constrictions (myogenic response) in parenchymal arterioles of BPV mice. While sensory stimulus-evoked dilations (neurovascular coupling) were amplified at higher BP levels in control mice, this pressure-dependent effect was abolished in BPV mice. Our findings indicate that chronic BP fluctuations impair vascular function within the neurovascular complex and contribute to cognitive decline, emphasizing BPV as a critical factor in brain health.

INTRODUCTION

Dementia, the 7th leading global cause of mortality, presents as the predominant neurodegenerative complication in the elderly population. Notably, hypertension emerges as a primary risk factor for dementia[1,2]. Blood pressure (BP) regulation involves a complex interplay of central and peripheral mechanisms, finely attuned to acute and chronic stressors in maintaining physiological ranges. Perturbations in vascular function and structure (e.g., reactivity, vascular stiffness[3]), alterations in baroreflex sensitivity[4], and enhanced sympathetic activation[5] are recognized factors that disrupt BP balance. Blood pressure variability (BPV) (an index of BP *fluctuation or variation*), particularly in midlife, increases the risk for cognitive decline[6], end-organ damage[7], and cardiovascular events[7,8]. Increased BPV also serves as an early predictor of hypertension[9]. BPV delineates fluctuations across various measurement periods from very short-term (beat-to-beat) to long-term (months or years[10]).

Given evidence that elevated BPV can precede hypertension[11], a modifiable risk factor in the setting of vascular cognitive impairment and dementia, understanding the drivers and cellular targets of BPV is essential. Unlike hypertension, BP fluctuations often elude detection in screening practices conducted in clinical settings, which rely on singular or averaged BP measurements[12]. The absence of a gold standard for BPV indexing[13] and limited insights into the magnitude and frequencies of impactful BP fluctuations in disease conditions further compound this issue. Additionally, the absence of suitable animal models has limited the understanding of how this overlooked variable may impact brain health. In this study, we sought to establish an innovative murine model of BPV and to interrogate the impact of large BP fluctuations on cardiovascular and neurovascular outcomes.

Cerebral blood flow (CBF) is tightly regulated by diverse signaling processes, including the interaction of cellular elements comprising the neurovascular complex, which include endothelial cells, vascular smooth muscle cells, pericytes, astrocytes, neurons, and microglia[14,15]. Mechanisms governing CBF operate under both steady-state conditions (e.g., cerebral autoregulation (CA), humoral processes, chemoregulation) and in response to local neuronal activity (e.g., neurovascular coupling (NVC))[16]. Evidence suggests that sustained hypertension adversely affects the functional integrity of the neurovascular complex[17-19], compromises cerebral perfusion[17,18] and contributes to cognitive decline[18]. However, the impact of large BP fluctuations on steady-state or activity-evoked CBF changes remains poorly understood.

Chronic hypertension leads to adaptive processes (e.g., vascular remodeling[20,21]) and a rightward shift in the cerebral autoregulation (CA) curve[22], heightening vulnerability to ischemia at low BP while shielding the brain from hyperperfusion at high pressure. In humans, hypertension and BPV have been associated with white matter hyperintensities[23-25] and microbleeds[26-28]. Intriguingly, the impact of BPV (prior to hypertension onset) on cerebrovascular function and neurovascular outputs has received little attention.

Using an innovative murine model of BPV, in the absence of overt hypertension, combined with *in vivo* two-photon imaging, we show that chronic BP fluctuations lead to microvascular dysfunction (e.g., enhanced parenchymal arteriole myogenic responses) and a blunted NVC response. In addition, mice subjected to chronic BPV showed poor cognitive performance. These findings underscore the pivotal role of dysregulated BP events in brain health and function.

METHODS

Animals

All experiments were conducted in middle-aged (12-15-month-old) male C57BL6 mice (Jackson Laboratories) under protocols approved by the Institutional Animal Care and Use Committee of Augusta University (AU). Mice were housed at 20-22°C under a 12hr:12hr light-dark cycle with *ad libitum* access to food and water. Female mice were not included in the present study due to high post-surgery mortality observed in 12-14-month-old mice following complex procedures. To minimized confounding effects of differential survival and to establish foundational data for this model, we restricted the investigation to male mice.

Craniotomy surgery for chronic window

Surgeries were conducted using the aseptic technique. Animals were injected with dexamethasone and meloxicam 2-4 hours before surgery to prevent edema and/or inflammation. General anesthesia was induced with isoflurane (2%) and following loss of reflex, hair was removed from the scalp and the mouse was transferred to a sterile field. A single injection of ketamine/dexdomitor (60 mg/kg/0.5mg/kg) was administered to maintain anesthesia in the sterile field. The scalp was scrubbed with betadine/alcohol (3 times each, alternating). A scalp incision was made (~1 cm). A small aluminum head holder (300 mg) was fixed to the skull using cyanoacrylate glue followed by dental cement and a small craniotomy opened over the cortex. The bone flap was removed. A glass coverslip (3 mm) was glued to a 4 mm coverslip and placed into the craniotomy with the inner glass touching the cortex. The edges of the coverslip were then

sealed with cyanoacrylate glue followed by dental cement covering everything including the wound margins.

Telemetry and iPrecio pump implantation surgery

Following a 3-week recovery period after craniotomy surgery, mice were implanted with a programmable pump (iPrecio, SMP-310R) and a biotelemetry transmitter device (PA-C10, Data Science International). Mice underwent brief anesthesia in a small chamber using 5% isoflurane for induction, followed by maintenance of anesthesia via a nose mask with 1.5-2% isoflurane. The neck fur was carefully clipped on both the anterior and posterior sides. Subsequently, mice were placed in a sterile field in a ventrally recumbent position, and a 1.5 to 2 cm horizontal incision was made. The pump and biotelemetry transmitter device were then implanted subcutaneously. The pump catheter was trimmed to 0.5 cm for subcutaneous drug delivery, while the telemeter catheter was tunneled subcutaneously over the shoulder, with its tip positioned within the left carotid artery. Closure of incisions was performed using 5-0 sutures, after which the mice were gradually brought out of anesthesia. It is important to note that due to the complexity of the surgeries involved, mice used for behavioral studies were not implanted with a telemetry catheter or cranial window. However, these mice were individually housed to simulate the conditions of the telemetry cohort.

Blood pressure assessment and BPV induction

After recovery from surgery, mice were housed individually in standard mouse cages under the conditions described above and assigned to a control or experimental BPV group. During this recovery period (~7 days), both groups were infused with saline to determine baseline cardiovascular parameters. Blood pressure signals encompassing mean arterial pressure (MAP), systolic blood pressure (SBP), diastolic blood pressure (DBP), heart rate (HR), and pulse pressure (PP) (determined from the difference between the SBP and DBP) were continuously sampled at 250 Hz for 10 seconds and collected every 30 seconds, for 24 hours per day. Once a baseline MAP was established, the saline in the infusion pump (in the BPV group) was substituted with angiotensin II (Ang II, Sigma Aldrich, A9525) and administered intermittently at a calculated dose of 3.1 μg/hour (every 3-4 hours) for 25 days.

Controls receiving Ang II: To facilitate between-group comparisons (control vs BPV), a cohort of control mice were subjected to the same pump infusion parameters as BPV mice but for shorter durations receiving Ang II infusions on days 3-5 and, then again, on days 21-25 of the experimental protocol. This paradigm was used for experiments assessing pressure-evoked

responses, including bradycardic reflex, myogenic response, and functional hyperemia at high BP.

BPV induction with norepinephrine: To validate the intermittent infusion protocol as an effective method for inducing significant BPV and not limited to Ang II, a separate cohort of mice received norepinephrine (NE, 45 µg/kg/min) using the same subcutaneous delivery protocol (2 µL every 4 hours).

Two-photon imaging

On the day of two-photon imaging acquisition, a mouse was anesthetized with chlorprothixene (0.04 cc) and a low dose of isoflurane (≤0.8%); a protocol to mildly sedate mice[29]. A retro-orbital injection of Texas red (70kDa dextran, 5% [wt/vol] in saline, 40 µl) was administered to label blood vessels. The mouse was head-fixed and a picospritzer (positioned on the contralateral hemisphere intended for imaging) was used to deliver a puff of air for whisker stimulation (WS) at a rate of 10 Hz for 20 seconds repeated six to eight times with ~ 90-second delay between each WS during an imaging session. Imaging sessions were conducted 106 ± 3.6 µm below the brain's surface while pump infusion was *off* (low BP period) and again during Ang II infusions (high BP period). Images were collected at a rate of 3.75 frames/second.

Behavioral studies

Behavioral tasks were performed by an experimenter at the AU small animal behavioral core (SABC), who was blinded to the experimental protocol. BPV mice were subjected to behavioral tests at two time points. First, during the saline infusion period, with observations considered as baseline, and second, 25-26 days post-Ang II infusions. About 30 minutes before training and testing, animals were brought to the testing room to acclimate. Animals remained in the laboratory for 15 minutes following study completion. To eliminate olfactory cues, animal droppings were removed, and the space and objects were cleaned (dilute 50% (vol/vol) ethanol solution) between sessions where appropriate.

Novel object recognition (NOR) task. Animal behavior was assessed using the previously described NOR task procedure[30]. Animals were acclimated and then familiarized with an opaque plastic chamber (78.7 cm x 39.4 cm x 31.7 cm) containing bedding for 10 minutes. The next day, a training session involved animals exploring two identical objects for 10 minutes before returning to their home cages. Object recognition was assessed one hour later by placing an animal in the NOR apparatus with a familiar object and a new or novel object for 10 minutes. The objects'

positions and roles (familiar or novel) were randomly assigned. Objects were positioned about 40 cm apart, 19.3 cm from the two short walls and 19.3 cm from the two long walls of the chamber. Exploration of an object was defined as direct interaction with nostrils or head position towards the object at a distance ≤ 2 cm. For data inclusion, a mouse had to explore an object for at least 4 seconds and spend a minimum of 10 seconds of total object exploration. Recognition index was calculated using the formula: $Recognition\ Index = \frac{(time\ spent\ at\ novel\ object\ )}{(time\ spent\ at\ novel + familiar\ objects)}$. The discrimination index was calculated as: $Discrimination\ Ratio = \frac{(time\ spent\ at\ novel - familiar\ object)}{(time\ spent\ at\ novel + familiar\ objects)}$. The one-hour delay for testing was determined based on earlier NOR tests assessing the cohort's recognition capacity at one, four, and 24-hour delays. The animals exhibited normal recognition capacity with a one-hour delay but failed at 4- and 24-hour delays. Hence, the one-hour delay was selected for subsequent tests.

*Y-maze***.** Y-maze tasks were performed twenty-four hours after NOR tasks. The Y-maze consisted of three arms (35.4 cm long, 9.9 cm wide with a height of 13.8 cm). Spontaneous alternation behavior was assessed by randomly placing mice in one of the three arms and allowed to explore for 10 minutes. Arm entries were visually scored into a series where a triplet set of arm entries constituted an alternation. An alternation was defined as successive consecutive entries into three different arms, and maximum alternations as the total number of arm entries minus 2. Percent alternation was calculated as the proportion of true alternations out of maximum alternations ((# of true alternations/# of maximum alternations) x 100).

Data analysis.

Two-day averaged values of 24-hour or 12-hour (active and inactive period) BP variables were compared to a baseline phase corresponding to saline infusion (~ 5 days). BPV was calculated using the average real variability (ARV) index ($\mathrm{ARV} = \frac{1}{\mathrm{N}-1}\sum_{\mathrm{K}=1}^{\mathrm{N}-1}\mathrm{x}|\mathrm{BP}_{\mathrm{K}+1} - \mathrm{BP}_{\mathrm{K}}|$) where K is the order of measurements and N denotes the number of BP readings. Absolute BP values were extracted every 15 minutes and averaged for the hour. The coefficient of variation (CV) was also used to calculate BPV. CV was calculated as the ratio of the standard deviation of hourly BP averages to the 24-hour BP average ($\mathrm{CV} = \frac{\text{Standard Deviation (Hourly BP Average)}}{\text{24 Hour BP Average}}$). Similar to BP variables, two-day averages of 24-hour and 12-hour ARV and CV were compared to the average value of the last 5 days during the baseline phase. Parenchymal arteriole diameter responses to changes in MAP (myogenic responses) and whisker stimulation were analyzed using MatLab and ImageJ[31,32]. Simple linear regression determined from the relationship of SBP

167 and HR assessed bradycardic responses; MAP and arteriole diameter changes assessed
168 myogenic reactivity. For neurovascular coupling experiments, the baseline was defined as 30
169 frames before stimulus onset. The stimulus-response comprised 100 frames encompassing the
170 20-second stimulus and the first 6 seconds post-stimulus. Six to eight WS events were averaged
171 for each run and responses were normalized to the baseline average.
172
173 *Exclusion Criteria*: Mice that died prematurely (before treatment onset) or exhibited abnormally
174 elevated or low blood pressures following telemetry surgery, likely due to surgical complications,
175 were excluded from the study.
176
177 During two-photon imaging sessions, we observed unexplained, random transient dilatory events
178 (**Supplemental Figure 1B, D**) occurring in both control and BPV mice across low- and high-BP
179 periods. Because similar random dilations have been documented in other mouse strains under
180 comparable *in vivo* imaging conditions, these events may be attributed to the effects of the
181 sedative. To isolate pressure-evoked parenchymal arteriole responses in the myogenic studies
182 (**Figure 5**), transient dilatory events associated with baseline tone were excluded from the
183 analysis, **Supplemental Figure 1F**.
184
185 *Study Limitations*: Experiments involving control and BPV mice were conducted across different
186 seasons, raising the possibility for seasonal influences[45,46]. To account for this, seven additional
187 control mice were included to the original thirteen control mice, **Supplemental Figure 2**. Six of
188 these mice underwent identical treatment but were allocated to a separate branch of the study
189 and did not receive chronic cranial window implantation−a procedure that does not significantly
190 affect BP, **Supplemental Figure 2A**. No differences in 24-hour averaged MAP were observed
191 between control mice when grouped categorized by Georgia's seasonal climate Fall-Winter
192 (October-April) vs Spring-Summer (May-September), **Supplemental Figure 2B**. Given the
193 absence of seasonal effects on BP and the fact that mice were sourced from two independent
194 suppliers (Jackson Laboratory and the National Institute of Aging Aged Colonies), we attribute
195 our observations primarily to treatment effects.
196
197 GraphPad Prism 10 software (GraphPad Software, La Jolla, CA) was used for all statistical
198 analyses. Values are expressed as mean ± SEM. A minimum of three mice was used for each
199 experimental data set, and the specific sample size (n) is defined in figure legends. Data was
200 tested for normal distribution, and statistical tests were used accordingly. Differences between

two means within groups were determined using paired Student's *t*-test. Differences between groups were determined using Student's unpaired *t*-test or two-way ANOVA with corresponding multiple comparison *post hoc* test specified in figure legends. Statistical significance was tested at a 95% ($P < 0.05$) confidence level denoted with the corresponding symbol in figure legends.

RESULTS

Pulsatile Ang II infusion-induced changes in blood pressure

We developed a novel murine model of high BPV using the experimental design shown in **Figure 1A**. The protocol consisted of a baseline phase (~5 days), corresponding to saline infusions in all mice, followed by a treatment phase (~20-25 days), where mice were either left on saline (control group) or subjected to robust BP transients induced via Ang II infusions (BPV group). Subcutaneous pumps were programmed to infuse 2 µL 6-8 times per day, with infusion periods corresponding to 1 hour every 3-4 hours (depending on the number of pulses), **Figure 1B**, right panel.

During the pump-*off* periods, BP corresponded to 97±2.0 mmHg and 91±1.9 mmHg for MAP, 113±2.6 mmHg and 105±2.6 mmHg for SBP, 80±1.7 mmHg and 78±1.7 mmHg for DBP, and 34±1.3 mmHg and 27±1.8 mmHg for PP, for mice with pumps infusing saline vs. Ang II, respectively (**Figure 1C**)**.** During the pump-*on* period, saline infusion did not change BP. However, Ang II infusions evoked significant BP transients corresponding to ∆37±3.9 mmHg (P<0.0001) for MAP, ∆70±3.0 mmHg (P<0.0001) for SBP, ∆29±4.1 mmHg (P<0.0001) for DBP, and ∆28±3.0 mmHg (P<0.0001) for PP, **Figure 1C**. Note that large dynamic activity-induced BP changes were apparent during both saline- and Ang II-infusions, **Figure 1B.** Despite robust BP transients, 20 days of treatment minimally affected the 24-hour averages (vs Baseline) in all cardiovascular variables, **Figure 1D**. The delta BP (Baseline vs Day 20) for MAP was -1±2.0 mmHg and 6±2.4 mmHg for control and BPV mice, respectively (**Figure 1D**). While the SBP in BPV mice significantly increased ∆9±2.9 mmHg (P=0.0088), mice remained within the lower range of high BP (131±4.4 mmHg). Additionally, prior to treatment, the baseline DBP in BPV was significantly lower than in control mice (P=0.0108), **Figure 1D**.

Blood pressure exhibits a circadian rhythm that is not discernible in minute-to-minute traces, (**Figure 1B**) but remains intact in both controls and BPV mice when analyzed in 1-hour averages, **Supplemental Figure 3C-D**. Thus, cardiovascular variables were assessed during the active (dark) and inactive (light) phases of the mouse 12:12 hr cycle. Consistent with the unchanged 24-

235 hour average for MAP, there were minimal changes in the averaged BP corresponding to the daily
236 inactive and active periods for control and BPV mice, **Figure 2A-D**. Compared to controls, the
237 DBP of the BPV group tended to be lower but not significant (P=0.09), **Figure 2C**. However,
238 beginning on day 7 of treatment, BPV (vs control) mice exhibited significantly higher PP during
239 the inactive period, **Figure 2D**. These data suggest a compensatory mechanism that maintains
240 MAP within physiological ranges, albeit with elevated PP in BPV mice.
241
242 **Pulsatile Ang II infusion induced high BPV**
243 Having achieved minimal changes in the 24-hour average MAP, yet with prominent BP
244 fluctuations, we quantified blood pressure variability (BPV) over time. Two indices of BPV were
245 assessed: the average real variability (ARV), defined as the absolute difference between
246 consecutive BP measurements, and the coefficient of variation (CV), defined as the ratio of the
247 standard deviation to mean BP. A significant increase in BPV was observed in the BPV group
248 over time relative to baseline, despite stable 24-hour BP averages. During the active period, ARV
249 was significantly increased by day 3 and remained increased throughout the protocol, reaching
250 16.4 ± 0.66 mmHg (P=0.04) for SBP and 8.12 ± 0.71 mmHg (P=0.04) for PP, **Table 1A**. Similarly,
251 during the inactive period, ARV was significantly increased by day 3 and persisted, with values of
252 13.4 ± 0.33 mmHg (P<0.01) for MAP, 17.3 ± 0.48 mmHg (P=0.02) for SBP, 11.3 ± 0.47 mmHg
253 (P<0.01) for DBP, and 7.9 ± 0.55 mmHg (P=0.04) for PP (**Table 1B**) with SBP as the main variable
254 driving BPV increases in this model. BPV indices using CV, based on hourly BP averages over
255 24 hours, were significantly increased from day 1 of treatment across all cardiovascular variables
256 during both the inactive and active periods, except for DBP of the active period, which increased
257 on day 3, **Supplement Table 1**.
258
259 **Autonomic function in BPV mice**
260 To compare pressure-induced bradycardic responses between BPV and control mice at both
261 early and later treatment stages, a cohort of control mice received Ang II infusion on days 3-5
262 (early phase) (**Supplemental Figure 4**) and days 21-25 (late phase) thereby transiently
263 increasing BP. Ang II evoked significant increases in SBP in both the control and BPV groups
264 which were accompanied by a pronounced bradycardic response, **Figure 3A**. For a single
265 infusion-evoked BP peak, changes in HR were -Δ291±34 bpm (P<0.0001) and -Δ304±17 bpm
266 (P<0.0001) for control and BPV mice, respectively (**Figure 3B**). While each Ang II infusion evoked
267 significant bradycardic responses, the 24-hour HR average was not significantly altered,

corresponding to 612±7 and 585±12 bpm for baseline and 570±25 and 546±8 bpm at day 20, for control and BPV mice, respectively, **Figure 3C**.

To assess whether chronic BP fluctuations affect the baroreflex response, we compared the slopes extracted from linear regression of SBP vs HR, focusing on within-group differences, **Figure 3D-G**. Comparisons were conducted over a 100-minute window surrounding a single Ang II-evoked BP pulse (20 minutes before and after 60-minute pulse), occurring during both the active and inactive periods, as well as between the early and late treatment phases. Linear regression analysis of SBP vs HR during Ang II infusion revealed no significant differences in the control group over time (Early vs Late), **Figure 3D, F.** However, the BPV group exhibited a significant reduction in the bradycardic response, indicated by flatter negative slopes during both the inactive ($P<0.0001$) and active periods ($P<0.001$) (**Figure 3E, G**). These data suggest that chronic (~25 days) BPV diminishes bradycardic responses, indicative of suppressed autonomic function.

Pulsatile Norepinephrine infusion induced BPV

To determine whether the observed cardiovascular effects of BPV were limited to Ang II, norepinephrine (NE, 45 µg/kg/min) was utilized as an alternative agent to induce BP variations, **Figure 4**. The NE dosage was titrated to match Ang II-induced BP transient pulse levels (150-200 mmHg, SBP) using the same subcutaneous delivery protocol (pump on for 1 hour every 4 hours) resulting in 6 pulses/day, **Figure 4A**. Similar to Ang II treated mice, NE-treated mice exhibited minimal changes in the 24-hr average MAP throughout the 20-day treatment, **Figure 4B**. While there was a trend towards increased ARV ($P=0.08$), it did not reach significance, **Figure 4C** left panel. However, CV, another BPV index, was significantly increased by day 3 ($P=0.02$) of the treatment, **Figure 4C** right panel.

In contrast to the bradycardic response observed during Ang II-induced BP elevations, NE-induced BP pulses triggered a tachycardic response (**Figure 4A**), with significant positive correlation between SBP and HR appearing during the early phase in the treatment (Inactive period, $P<0.0001$; Active period, $P=0.0002$), **Figure 4D**. These data validate the intermittent infusion protocol as an effective method for inducing significant BPV while preserving normal 24hr MAP. However, due to fundamental differences in bradycardic responses and the presence of off-target effects, the physiological actions of this vasopressor agent are not directly comparable to those of Ang II. These results underscore the necessity of careful vasopressor selection to mitigate off-target effects.

302 **Chronic BPV enhanced parenchymal arteriole myogenic responses**

303 CBF regulation involves complex processes that maintain the metabolic needs of working
304 neurons. These include mechanisms active at baseline (e.g., cerebral autoregulation[16] and
305 endothelial cell-mediated signaling[33]) and those involved in activity-mediated increases in CBF or
306 neurovascular coupling (NVC)[14]. To assess if BPV impacts the functional integrity of the
307 neurovascular complex, we measured parenchymal arteriole responses to acute BP increases
308 and determined if BP itself altered the sensory-evoked arteriole response. For these studies, *in*
309 *vivo* two-photon imaging was combined with BP measurements via telemetry, **Figures 5** and **6**.
310

311 To determine the impact of acute BP changes on the microcirculation, we simultaneously tracked
312 parenchymal arteriole diameter changes before pump infusion onset (Low BP), and during Ang II
313 infusions (High BP), **Figure 5E**. For these experiments, and prior to the imaging session, the
314 pump reservoir for the control group was switched from saline to Ang II. Imaging was conducted
315 at similar cortical depths (~ layer 1/2 border of the somatosensory cortex) corresponding to
316 106±11.6 μm and 102±4.3 μm for control and BPV mice, respectively, **Figure 5B.** Arteriole
317 diameters measured at baseline (Low BP) were comparable between groups, corresponding to
318 18.6±1.1 μm and 19±1.0 μm for controls and BPV mice, respectively, **Figure 5C**. Upon mild
319 sedation resting BP dropped by -23±3.6 mmHg and -31±4.4 mmHg for the control and BPV group,
320 respectively (not shown). However, BP values remained within the putative cerebral
321 autoregulation plateau range throughout two-photon imaging sessions and were comparable
322 between groups. During the pump infusion period (High BP), the BP increased from 68±4.2 to
323 102±5.9 mmHg for controls ($P<0.0001$) and from 59±4.5 to 96±6.4 mmHg for BPV mice
324 ($P<0.0001$), **Figure 5D.**
325

326 To quantify *in vivo* pressure-evoked diameter changes (myogenic responses), we compared the
327 slopes extracted from the linear regression of MAP vs parenchymal arteriole diameter measured
328 throughout the acquisition session, **Figure 5E-G**. The steeper negative slope observed in BPV
329 mice compared to controls indicates significantly increased parenchymal arteriole reactivity to BP
330 changes ($P=0.0118$), **Figure 5H**. However, because BPV mice exhibited lower baseline BP,
331 although not significantly different from controls ($P=0.18$, **Figure 5D**), we examined whether
332 differences in pressure range (i.e. the change in pressure between low and high BP intervals)
333 contributed to the steeper slopes observed in BPV mice. **Figure 5I** illustrates the relationship
334 between the lowest BP recorded during the acquisition period and the slope derived from the
335 MAP-diameter linear regression analysis. Dashed lines represent the percent change in MAP

336 relative to the minimal averaged BP recorded at the start of the imaging session. BPV mice
337 showed a trend for greater percent change in BP (%Δ61±5.4 mmHg vs %Δ47±4.0 mmHg for
338 control mice, P=0.06; **Figure 5I**, insert). However, the average BP range in control mice was still
339 sufficient for establishing a correlation between BP and diameter, supporting the interpretation
340 that differences in myogenic response stem from intrinsic vascular reactivity rather than limitations
341 in the BP range.
342
343 The static cerebral autoregulation curve (CA), originally described by Lassen in 1959, is
344 characterized by a plateau phase in the MAP-CBF relationship, sandwiched between lower and
345 upper limit ranges[33]. However, the shape of the curve has been challenged[34], with evidence
346 suggesting a narrower plateau range and potential dilatory phases as BP deviates from this
347 range[35]. To investigate pressure-diameter relationships in our cohort of mice, we analyzed
348 parenchymal arterioles from control and BPV mice. As shown in **Figure 5J**, arterioles of both
349 groups exhibited significant increases in tone (P<0.0001) as pressure rose from ~50 to 125
350 mmHg. When slopes from segmented regression analyses were compared across autoregulatory
351 limits and plateau ranges[35], our data revealed a significant decrease in arteriole diameter
352 (P=0.0015) in control mice at pressures <50 mmHg (**Figure 5K**). Within the putative CA plateau
353 range (51-100 mmHg)[35], arterioles from both groups showed significant constrictions (P=0.01 for
354 controls; P<0.0001 for BPV mice, **Figure 5L**), with steeper slopes observed in BPV arterioles
355 (P<0.0001). At pressures >100 mmHg, BPV arterioles exhibited significant arterial dilations
356 (P<0.001), whereas control arterioles maintained constrictions (P<0.001, **Figure 5M**). Together,
357 these data suggest a leftward shift in the CA curve of BPV mice, characterized by enhanced
358 myogenic constrictions at comparable pressures and significant arterial dilations at higher
359 pressures where controls arterioles maintain tone, **Figure 5N**.
360
361 Previous studies have shown directional sensitivity in parenchymal arteriole responses, whereby
362 increases in MAP evoke more efficient responses as compared to decreases in MAP. Thus, we
363 separated and quantified diameter changes evoked by BP transitions from Low-to-High (increase
364 MAP) and High-to-Low BP (decrease MAP), **Supplemental Figure 5A-F**. Ang II infusion evoked
365 similar increases in MAP when BP transitioned from Low-to-High Δ27±3.6 mmHg in controls and
366 Δ25±3.6 mmHg in BPV mice, **Supplemental Figure 5A**. In addition, MAP decreases were
367 comparable between groups (-Δ21±2.8 mmHg for controls and -Δ25±3.1 mmHg for BPV mice)
368 upon cessation of pump infusion (High-to-Low), **Supplemental Figure 5D**. The significantly
369 steeper negative slopes in BPV arterioles relative to controls (P=0.0117, Low-to-High)

370 (**Supplemental Figure 5C**) demonstrate increased parenchymal arteriole constriction to
371 increases in MAP. Conversely, we also observed steeper negative slopes in BPV arterioles
372 compared to controls (P=0.0044, High-to-Low) (**Supplemental Figure 5F**) with decreases in MAP
373 suggestive of enhanced arteriole dilations. Collectively, these findings indicate that chronic BPV
374 heightens the responsiveness of parenchymal arterioles to acute BP fluctuations.
375
376 **Impaired NVC in high BPV mice**
377 Because mechanisms underlying baseline CBF regulation differ from those evoked during the
378 functional hyperemia response, we assessed whether chronic BPV affected functional-evoked
379 outputs or neurovascular coupling (NVC). Functional hyperemia was assessed using two-photon
380 imaging and evoked using air puffs to stimulate mouse whiskers. Blood pressure measurements
381 were simultaneously measured via telemetry, **Figure 6A**. While sensory-evoked vascular
382 responses are commonly used as a proxy for neuronal activation and function[18,34], few studies
383 have considered (or reported) BP during these *in vivo* protocols. Thus, we asked if chronic and
384 acute BP fluctuations alter the NVC response at the level of parenchymal arterioles, **Figure 6B**.
385 NVC responses were compared during low and high BP periods corresponding to pumps being
386 *off* or *on*, respectively, **Figure 6E**.
387
388 The average baseline (low BP) MAP was 78±2.5 mmHg and 71.0±3.4 for the control and BPV
389 group, respectively, **Figure 6C**. Imaging was conducted at similar cortical depths within ~ layers
390 1/2 border of the somatosensory cortex, corresponding to 107±1.0 μm and 96±0.4 μm for control
391 and BPV arterioles, respectively, **Figure 6D.** To compare NVC responses at low and high BP, the
392 pump reservoir for the control group was switched from saline to Ang II. Ang II infusion evoked
393 significant (and comparable) increases in MAP, corresponding to 92±3.5 mmHg for controls and
394 92±5.7 mmHg for BPV mice, **Figure 6C**. **Figure 6E**, show a representative trace of the
395 simultaneous MAP and arteriole diameter changes; WS denotes the stimulation period and "a"
396 and "b" the timepoint from where diameters where measured before and after the stimulus,
397 respectively and summarized in **Figure 6F**. Whisker stimulation caused significant dilations (vs.
398 baseline) in all groups, regardless of MAP, **Figure 6G, H**. However, at higher BP, the magnitude
399 of the NVC response in control mice was greater (P<0.0001, high BP vs low BP). Notably, this
400 pressure-dependent response was abrogated (P=0.60) in the BPV group, **Figure 6G, H.** A closer
401 look at the post-stimulus recovery phase showed a faster recovery rate (k = -0.45) for
402 parenchymal arterioles of BPV mice during high BP periods compared to controls (P<0.0001),
403 **Figure 6I**. These data revealed an acute pressure-dependent effect in control mice, with higher

404 pressures resulting in greater sensory-evoked dilations. Additionally, the data shows that chronic
405 BP fluctuations abrogated the pressure-dependent effects observed in control mice.
406
407 **Cognitive decline in high BPV mice**
408 Given impaired neurovascular outputs and the established association between high BPV and
409 cognitive decline[35], we used the NOR and Y-maze tests to assess cognitive performance. Mice
410 were subjected to behavioral testing during the saline-infused period and following 25 days of
411 BPV (via Ang II infusions). Using NOR, a significant decrease in the recognition index (P=0.006)
412 and discriminatory index (P=0.006) was observed (**Figure 7A**), supporting impaired recognition
413 memory. No differences were observed in the short-term spatial working memory assessed via
414 Y-maze alternation (P=0.25), **Figure 7B**.
415
416 Mice activity levels were evaluated as another aspect of behavior. Throughout the study, activity
417 remained consistently higher during the active vs inactive periods (P=0.049 for control, P=0.0287
418 for BPV), **Figure 7C**. However, following 23-25 days of treatment (Late), BPV mice exhibited a
419 significant reduction in activity when the pump was *on*. This decline was evident in the 24-hour
420 average data (P=0.0111, **Figure 7D**), as well as during the active period of the 12-hour activity
421 averages (pump *on* vs *off*, P=0.0122, **Figure 7F**). These data support that mice subjected to
422 chronic BPV become less active when the BP increases or the pump status is *on*. Notably, while
423 the infusion protocol preserves BP-related circadian rhythms, 25 days of chronic BPV negatively
424 impacts both recognition memory and overall activity levels.
425
426 **DISCUSSION**
427 BPV has emerged as a risk factor for cognitive decline, yet its impact on brain function remains
428 poorly understood. Here, we introduce a novel murine model of BPV, where pulsatile BP
429 increases were induced via Ang II infusions without hypertension. Using *in vivo* two-photon
430 imaging, we provide evidence of altered vascular function in mice subjected to chronic BP
431 fluctuations. In BPV mice, parenchymal arterioles (<30 μm in diameter) exhibited enhanced
432 myogenic reactivity. In addition, chronic BPV impaired neurovascular outputs and cognitive
433 function. Notably, the NVC response in control mice was pressure-dependent, with greater
434 magnitudes observed when the arterial BP was increased−a relationship that was abolished in
435 mice exposed to chronic BPV. These findings suggest that chronic BPV targets multiple
436 physiological processes (e.g., bradycardic reflex, myogenic reactivity, neurovascular coupling)
437 reinforcing its role as a critical risk factor for brain health.

438 Our goal was to induce rapid transient blood pressure pulses that significantly increased BPV,
439 while maintaining a stable 24hr average blood pressure. Ang II was selected as a pressor due to
440 its potent vasoconstrictive properties and short half-life[36]. The subcutaneous dose was carefully
441 titrated to induce BP elevations reaching physiological high levels (150−200 mmHg, SBP),
442 achievable in non-diseased conditions and comparable to doses used in miniosmotic pumps[37-39].
443 The precise mechanisms underlying increased BPV remain unclear, though vascular dysfunction
444 and arterial stiffness have been postulated as contributing factors[40]. Age is strongly correlated
445 with arterial stiffness and isolated systolic hypertension[41]. Notably, SBP was modestly increased
446 downstream of BPV in the current model, **Figure 1D**. In the BPV cohort, six out of eight mice
447 exhibited an SBP increase of >Δ10 mmHg compared to baseline (**Figure 1D**), suggesting that
448 elevated BPV may contribute to the early onset of systolic hypertension. Given that isolated
449 systolic hypertension is a risk factor for overt hypertension[42] and BPV precedes hypertension[11],
450 prolonged BPV beyond the 25-day treatment period could potentially lead to hypertension.
451 Furthermore, we anticipate that sustained BPV and its resultant hypertension may drive cardiac
452 remodeling, specifically, left ventricular hypertrophy. These findings underscore the need for
453 future studies to investigate the long-term effects of BPV on cardiac morphology.
454
455 We explored norepinephrine as an alternative agent to induce BP variations, **Figure 4**. Similar to
456 Ang II-infused mice, NE-treated mice exhibited a significant increase in BPV (i.e. increased CV)
457 while maintaining minimal changes in the 24-hr averaged MAP. However, NE-induced BP pulses
458 elicited a tachycardic response likely driven by NE stimulation of cardiac β1-adrenergic
459 receptors[43]. Notably, chronic NE administration exaggerated this tachycardic response, with a
460 steeper positive slope over time (Early vs Late; $P<0.0001$) during the Inactive period, **Figure 4D**.
461 Additionally, NE-treated mice exhibited signs of lethargy, impaired mobility, tachypnea, and an
462 increased rate of premature death beginning on day 11 of treatment. These findings emphasize
463 the need for further investigation into alternative BPV pressors, as each may exert distinct off-
464 target effects.
465
466 Our model underscores the importance of assessing BPV independently of average BP values.
467 Retrospective studies in primary care patients reveal BPV occurrences in both hypertensive and
468 non-hypertensive adults[44], establishing BPV as a critical yet modifiable risk factor, often
469 overlooked by standard in-office single BP measurements. In our model, the significantly higher
470 24-hour average PP in BPV mice suggests that PP is the most sensitive BP-related variable.
471 Compared to controls, BPV mice exhibited persistently lower DBP and higher PP during the

472 inactive period, indicative of a compensatory mechanism that maintained 24-hour MAP within
473 physiological ranges. However, other factors mitigating hypertension onset cannot be ruled out.
474
475 The autonomic nervous system (ANS) tightly regulates BP via changes in heart rate, systemic
476 vascular resistance, and stroke volume. Notably, the baroreflex plays a critical role in maintaining
477 cerebral perfusion pressure[47]. Acute BP elevations activate arterial baroreceptors, which inhibit
478 sympathetic outflow (via enhanced vagal activity) and reduce HR and peripheral vascular
479 resistance[47], thereby lowering arterial BP. However, to sustain relatively stable CBF, baroreflex-
480 mediated inhibition of sympathetic outflow and arteriole dilation is counterbalanced by the intrinsic
481 myogenic properties of the cerebral vasculature, which constricts in response to increases in
482 arterial BP. Dysregulation of these dynamic processes heightens the risk of both cerebral
483 hypoperfusion and hyperperfusion. Notably, impaired baroreflex sensitivity has been linked to
484 aging[48] and mild cognitive impairments[49].
485
486 In our model, chronic BPV significantly blunted the bradycardic response, suggestive of ANS
487 dysregulation, potentially driven by enhanced sympathetic activity, reduced parasympathetic
488 activity, or a combination of both. Previous studies indicate that chronic Ang II infusion suppresses
489 and resets baroreceptor sensitivity independently of the pressure effect, with partial reversal
490 occurring within 30 minutes post-Ang II infusion[50]. Unlike conventional sustained Ang II infusion
491 approaches (osmotic pump models), our protocol delivers Ang II intermittently at 3- or 4-hour
492 intervals. This regimen likely mitigates desensitization and Ang II receptor internalization, a
493 response well-documented in sustained infusion models[51,52]. Furthermore, the same Ang II dose
494 evoked comparable BP increases at the start and end of treatment. Thus, our results support
495 diminished baroreflex responses, aligning with previous reports linking elevated BPV to
496 autonomic dysregulation[53], though the underlying cellular mechanisms remain poorly understood.
497
498 Cerebral autoregulation serves as a protective mechanism against fluctuations in cerebral
499 perfusion pressure[22]. Vessels upstream from cerebral capillaries, including pial arteries[54-56] and
500 larger extracranial vessels[57-59], help buffer arterial pressure changes, thereby limiting excessive
501 variations in CBF. In response to chronic and sustained hypertension, parenchymal arterioles
502 exhibit enhanced reactivity to pressure increases[21,60,61]. This is further accompanied by arteriole
503 remodeling[21,62,63]. Although our model does not involve sustained hypertension, we present *in*
504 *vivo* evidence of heightened myogenic responses of parenchymal arterioles to both BP elevations

505 and reductions. These observations are particularly intriguing as they suggest potential adaptive
506 mechanisms in response to large blood pressure fluctuations.
507
508 Chronic BP elevations may drive upregulation of voltage-dependent calcium channels (VDCC),
509 or suppression of K^+ currents[64]. Cipolla et al., reported that parenchymal arterioles are
510 approximately 30-fold more sensitive to VDCC inhibition via nifedipine than middle cerebral
511 arteries[65]. Notably, VDCC expression increases in hypertension[66-72], and long-acting calcium
512 channel blockers (i.e., amlodipine), are among the most effective treatments for BPV [73,74]. In an
513 effort to mitigate excessive vasoconstriction and optimize blood flow, during periods of BP-
514 induced constrictions, vasodilatory signals may accumulate. Consequently, when BP decreases,
515 parenchymal arterioles in BPV mice may exhibit greater dilation compared to controls,
516 **Supplemental Figure 5F**. Augmented vasodilation has been reported as adaptive response in
517 rodent models of chronic hypoperfusion[75,76]. The dynamic nature of BP fluctuations in our model
518 (i.e. increases and decreases) uniquely allows observations of multiple processes occurring
519 concurrently (e.g. enhanced vasoconstrictions in response to high BP, and enhanced dilations
520 potentially resulting from vasoconstriction-evoked ischemia).
521
522 If this interpretation holds, our model may reflect conditions in which parenchymal arterioles
523 experience both high pressure and ischemia. The resulting heightened myogenic responses may
524 amplify diameter changes, potentially diminishing pressure buffering capacity and increasing
525 vulnerability to extreme BP fluctuations, predisposing brain tissue to episodic ischemia and/or
526 hyperperfusion. Future studies addressing the impact of BPV on capillary perfusion may provide
527 further insights into the link between BPV and brain pathology, including microbleeds[77,78].
528
529 Chronic BPV significantly blunted the NVC response to whisker stimulation. In control mice, NVC
530 exhibited a pressure-dependent effect, with greater response magnitudes observed at higher
531 arterial BP levels−an effect that was abolished in BPV mice. One possible explanation is that the
532 enhanced NVC response (under high BP conditions) in control mice stems from greater baseline
533 arteriole tone, facilitating a more efficient dilatory response to vasoactive signals released during
534 sensory-evoked stimuli. Conversely, the heightened reactivity of parenchymal arterioles to
535 intravascular pressure in BPV mice (**Figure 5H**) suggests a predominant vasoconstrictive state[79],
536 potentially accompanied by reduced availability of vasodilatory mediators involved in NVC (e.g.
537 nitric oxide, epoxyeicosatrienoic acids (EETs), cyclooxygenase-derived prostaglandins)[80,81].

538 Thus, the blunted NVC response observed during elevated BP periods in BPV mice may also
539 result from impaired vasodilation.
540
541 Additionally, upon termination of WS, vasoconstrictive mechanisms−exacerbated by elevated BP
542 are unmasked, leading to a faster recovery in arteriole diameter post-stimulus[82]. Another potential
543 explanation is a neuronal mechanism, where diminished neural activity or reduced release of
544 vasodilatory signals may contribute to the impaired NVC response. Further studies should
545 investigate the impact of high BPV on the neurovascular complex under awake conditions,
546 recognizing that factors such as activity and arousal[83,84], can elevate BP and potentially confound
547 pressure-dependent neurovascular effects.
548
549 Beyond blunting NVC, our study demonstrates that chronic BPV contributes to cognitive decline,
550 as evidenced by decreased discrimination and recognition indices in the NOR test. Clinical studies
551 have similarly linked elevated BPV to impairments across multiple cognitive domains, including
552 memory and executive function[85,86]. Post hoc analyses of the SPRINT MIND trial revealed that
553 patients with elevated BPV experienced the most rapid decline in processing speed[86].
554 Additionally, findings from the Alzheimer's Disease Neuroimaging Initiative indicated that greater
555 SBP variability correlated with poorer episodic memory performance[85].
556
557 To assess cognitive function, we employed the NOR test to evaluate episodic memory[87] and the
558 spontaneous Y maze test to assess short-term spatial memory[88]. Because telemetry systems
559 necessitated individual housing to avoid signal interference, all mice used in this study were
560 single-housed. Previous studies on C57BL/6 mice have reported conflicting effects of single
561 housing on learning and memory[89-91], with some suggesting stress-induced deficits and others
562 reporting no impact[92-95]. These discrepancies may stem from variables such as age at isolation
563 onset, duration of isolation, and behavioral test conditions. To minimize confounding factors, we
564 implemented stringent efforts to ensure consistency across all groups, including standardized
565 cage changes, food replenishment, and pump refills conducted on a single day between 1:00 and
566 4:00 PM Our results indicate that while 25 days of chronic BPV does not affect short-term spatial
567 memory, it significantly impairs episodic memory.
568
569 **Conclusions**
570 Our study demonstrates that high BPV disrupts cellular communication in the neurovascular
571 complex, contributing to cognitive decline. Importantly, our model elicited substantial BP

fluctuations while preventing the onset of hypertension, providing direct evidence of BPV's causal role in impaired neurovascular function. These findings support the inclusion of BPV assessment as a critical screening and diagnostic tool alongside conventional BP measurements to address cardiovascular and neurovascular risks. Moreover, the adaptable murine model developed in this study offers a robust framework for future investigations into BPV's impact on brain function.

ACKNOWLEDGMENTS

This research was supported by 1R56NS123644, 5R01NS123644 to JAF and 24POST1196351 AHA and 3R01NS097818-03S1 to PJM. We acknowledge the contributions of animals from the National Institutes of Aging. In addition, we thank Kathleen A. Coleman, and Cameron Folk, for their technical support in conducting telemetry and pump-related surgeries. We also thank Dr Alvin Terry and Daniel Beck the AU Small Animal Behavioral Core for their assistance with the behavioral cognitive tests. Diagrams created with Biorender.com

1. Baggeroer CE, Cambronero FE, Savan NA, Jefferson AL, Santisteban MM. Basic Mechanisms of Brain Injury and Cognitive Decline in Hypertension: Dementia Series. *Hypertension*. 2023. doi: 10.1161/HYPERTENSIONAHA.123.19939
2. Iadecola C, Yaffe K, Biller J, Bratzke LC, Faraci FM, Gorelick PB, Gulati M, Kamel H, Knopman DS, Launer LJ, et al. Impact of Hypertension on Cognitive Function: A Scientific Statement From the American Heart Association. *Hypertension*. 2016;68:e67-e94. doi: 10.1161/HYP.0000000000000053
3. Boutouyrie P, Chowienczyk P, Humphrey JD, Mitchell GF. Arterial Stiffness and Cardiovascular Risk in Hypertension. *Circ Res*. 2021;128:864-886. doi: 10.1161/CIRCRESAHA.121.318061
4. Hesse C, Charkoudian N, Liu Z, Joyner MJ, Eisenach JH. Baroreflex sensitivity inversely correlates with ambulatory blood pressure in healthy normotensive humans. *Hypertension*. 2007;50:41-46. doi: 10.1161/HYPERTENSIONAHA.107.090308
5. de Leeuw PW, Bisognano JD, Bakris GL, Nadim MK, Haller H, Kroon AA, HT DE, Rheos Trial I. Sustained Reduction of Blood Pressure With Baroreceptor Activation Therapy: Results of the 6-Year Open Follow-Up. *Hypertension*. 2017;69:836-843. doi: 10.1161/HYPERTENSIONAHA.117.09086
6. Nagai M, Hoshide S, Ishikawa J, Shimada K, Kario K. Visit-to-visit blood pressure variations: new independent determinants for cognitive function in the elderly at high risk of cardiovascular disease. *J Hypertens*. 2012;30:1556-1563. doi: 10.1097/HJH.0b013e3283552735
7. Vishram JK, Dahlof B, Devereux RB, Ibsen H, Kjeldsen SE, Lindholm LH, Mancia G, Okin PM, Rothwell PM, Wachtell K, Olsen MH. Blood pressure variability predicts cardiovascular events independently of traditional cardiovascular risk factors and target organ damage: a LIFE substudy. *J Hypertens*. 2015;33:2422-2430. doi: 10.1097/HJH.0000000000000739
8. Ernst ME, Chowdhury EK, Beilin LJ, Margolis KL, Nelson MR, Wolfe R, Tonkin AM, Ryan J, Woods RL, McNeil JJ, et al. Long-Term Blood Pressure Variability and Risk of Cardiovascular Disease Events Among Community-Dwelling Elderly. *Hypertension*. 2020;76:1945-1952. doi: 10.1161/HYPERTENSIONAHA.120.16209
9. Bohm M, Schumacher H, Leong D, Mancia G, Unger T, Schmieder R, Custodis F, Diener HC, Laufs U, Lonn E, et al. Systolic blood pressure variation and mean heart rate is associated with cognitive dysfunction in patients with high cardiovascular risk. *Hypertension*. 2015;65:651-661. doi: 10.1161/HYPERTENSIONAHA.114.04568
10. Parati G, Stergiou GS, Dolan E, Bilo G. Blood pressure variability: clinical relevance and application. *J Clin Hypertens (Greenwich)*. 2018;20:1133-1137. doi: 10.1111/jch.13304
11. Ozkan G, Ulusoy S, Arici M, Derici U, Akpolat T, Sengul S, Yilmaz R, Erturk S, Arinsoy T, Deger SM, Erdem Y. Does Blood Pressure Variability Affect Hypertension Development in Prehypertensive Patients? *Am J Hypertens*. 2022;35:73-78. doi: 10.1093/ajh/hpab125
12. Schutte AE, Kollias A, Stergiou GS. Blood pressure and its variability: classic and novel measurement techniques. *Nature reviews Cardiology*. 2022;19:643-654. doi: 10.1038/s41569-022-00690-0
13. Del Giorno R, Balestra L, Heiniger PS, Gabutti L. Blood pressure variability with different measurement methods: Reliability and predictors. A proof of concept cross sectional study in elderly hypertensive hospitalized patients. *Medicine (Baltimore)*. 2019;98:e16347. doi: 10.1097/MD.0000000000016347
14. Iadecola C. The Neurovascular Unit Coming of Age: A Journey through Neurovascular Coupling in Health and Disease. *Neuron*. 2017;96:17-42. doi: 10.1016/j.neuron.2017.07.030
15. Schaeffer S, Iadecola C. Revisiting the neurovascular unit. *Nat Neurosci*. 2021;24:1198-1209. doi: 10.1038/s41593-021-00904-7

16. Claassen J, Thijssen DHJ, Panerai RB, Faraci FM. Regulation of cerebral blood flow in humans: physiology and clinical implications of autoregulation. *Physiol Rev*. 2021;101:1487-1559. doi: 10.1152/physrev.00022.2020
17. Capone C, Faraco G, Peterson JR, Coleman C, Anrather J, Milner TA, Pickel VM, Davisson RL, Iadecola C. Central cardiovascular circuits contribute to the neurovascular dysfunction in angiotensin II hypertension. *The Journal of neuroscience : the official journal of the Society for Neuroscience*. 2012;32:4878-4886. doi: 10.1523/JNEUROSCI.6262-11.2012
18. Faraco G, Sugiyama Y, Lane D, Garcia-Bonilla L, Chang H, Santisteban MM, Racchumi G, Murphy M, Van Rooijen N, Anrather J, Iadecola C. Perivascular macrophages mediate the neurovascular and cognitive dysfunction associated with hypertension. *J Clin Invest*. 2016;126:4674-4689. doi: 10.1172/JCI86950
19. Santisteban MM, Iadecola C, Carnevale D. Hypertension, Neurovascular Dysfunction, and Cognitive Impairment. *Hypertension*. 2023;80:22-34. doi: 10.1161/HYPERTENSIONAHA.122.18085
20. Izzard AS, Horton S, Heerkens EH, Shaw L, Heagerty AM. Middle cerebral artery structure and distensibility during developing and established phases of hypertension in the spontaneously hypertensive rat. *J Hypertens*. 2006;24:875-880. doi: 10.1097/01.hjh.0000222757.54111.06
21. Pires PW, Jackson WF, Dorrance AM. Regulation of myogenic tone and structure of parenchymal arterioles by hypertension and the mineralocorticoid receptor. *Am J Physiol Heart Circ Physiol*. 2015;309:H127-136. doi: 10.1152/ajpheart.00168.2015
22. Iadecola C, Davisson RL. Hypertension and cerebrovascular dysfunction. *Cell Metab*. 2008;7:476-484. doi: 10.1016/j.cmet.2008.03.010
23. van Dijk EJ, Breteler MM, Schmidt R, Berger K, Nilsson LG, Oudkerk M, Pajak A, Sans S, de Ridder M, Dufouil C, et al. The association between blood pressure, hypertension, and cerebral white matter lesions: cardiovascular determinants of dementia study. *Hypertension*. 2004;44:625-630. doi: 10.1161/01.HYP.0000145857.98904.20
24. Dufouil C, de Kersaint-Gilly A, Besancon V, Levy C, Auffray E, Brunnereau L, Alperovitch A, Tzourio C. Longitudinal study of blood pressure and white matter hyperintensities: the EVA MRI Cohort. *Neurology*. 2001;56:921-926. doi: 10.1212/wnl.56.7.921
25. Zhang B, Huo Y, Yang Z, Lv H, Wang Y, Feng J, Han Y, Wang H. Day to Day Blood Pressure Variability Associated With Cerebral Arterial Dilation and White Matter Hyperintensity. *Hypertension*. 2022;79:1455-1465. doi: 10.1161/HYPERTENSIONAHA.122.19269
26. Elmstahl S, Ellstrom K, Siennicki-Lantz A, Abul-Kasim K. Association between cerebral microbleeds and hypertension in the Swedish general population "Good Aging in Skane" study. *J Clin Hypertens (Greenwich)*. 2019;21:1099-1107. doi: 10.1111/jch.13606
27. Reddy ST, Savitz SI. Hypertension-Related Cerebral Microbleeds. *Case Rep Neurol*. 2020;12:266-269. doi: 10.1159/000508760
28. Liang C, Wang J, Feng M, Zhang N, Guo L. White matter changes, duration of hypertension, and age are associated with cerebral microbleeds in patients with different stages of hypertension. *Quantitative imaging in medicine and surgery*. 2022;12:119-130. doi: 10.21037/qims-21-28
29. O'Herron PJ, Hartmann DA, Xie K, Kara P, Shih AY. 3D optogenetic control of arteriole diameter in vivo. *eLife*. 2022;11. doi: 10.7554/eLife.72802
30. Callahan PM, Terry AV, Jr., Peitsch MC, Hoeng J, Koshibu K. Differential effects of alkaloids on memory in rodents. *Sci Rep*. 2021;11:9843. doi: 10.1038/s41598-021-89245-w
31. Chhatbar PY, Kara P. Improved blood velocity measurements with a hybrid image filtering and iterative Radon transform algorithm. *Frontiers in neuroscience*. 2013;7:106. doi: 10.3389/fnins.2013.00106

32. O'Herron P, Chhatbar PY, Levy M, Shen Z, Schramm AE, Lu Z, Kara P. Neural correlates of single-vessel haemodynamic responses in vivo. *Nature*. 2016;534:378-382. doi: 10.1038/nature17965
33. Longden TA, Dabertrand F, Koide M, Gonzales AL, Tykocki NR, Brayden JE, Hill-Eubanks D, Nelson MT. Capillary K(+)-sensing initiates retrograde hyperpolarization to increase local cerebral blood flow. *Nat Neurosci*. 2017;20:717-726. doi: 10.1038/nn.4533
34. Lecrux C, Toussay X, Kocharyan A, Fernandes P, Neupane S, Levesque M, Plaisier F, Shmuel A, Cauli B, Hamel E. Pyramidal neurons are "neurogenic hubs" in the neurovascular coupling response to whisker stimulation. *The Journal of neuroscience : the official journal of the Society for Neuroscience*. 2011;31:9836-9847. doi: 10.1523/JNEUROSCI.4943-10.2011
35. McGrath ER, Beiser AS, DeCarli C, Plourde KL, Vasan RS, Greenberg SM, Seshadri S. Blood pressure from mid- to late life and risk of incident dementia. *Neurology*. 2017;89:2447-2454. doi: 10.1212/WNL.0000000000004741
36. Al-Merani SA, Brooks DP, Chapman BJ, Munday KA. The half-lives of angiotensin II, angiotensin II-amide, angiotensin III, Sar1-Ala8-angiotensin II and renin in the circulatory system of the rat. *J Physiol*. 1978;278:471-490. doi: 10.1113/jphysiol.1978.sp012318
37. Zimmerman MC, Lazartigues E, Sharma RV, Davisson RL. Hypertension caused by angiotensin II infusion involves increased superoxide production in the central nervous system. *Circ Res*. 2004;95:210-216. doi: 10.1161/01.RES.0000135483.12297.e4
38. Nakagawa P, Nair AR, Agbor LN, Gomez J, Wu J, Zhang SY, Lu KT, Morgan DA, Rahmouni K, Grobe JL, Sigmund CD. Increased Susceptibility of Mice Lacking Renin-b to Angiotensin II-Induced Organ Damage. *Hypertension*. 2020;76:468-477. doi: 10.1161/HYPERTENSIONAHA.120.14972
39. Gonzalez-Villalobos RA, Seth DM, Satou R, Horton H, Ohashi N, Miyata K, Katsurada A, Tran DV, Kobori H, Navar LG. Intrarenal angiotensin II and angiotensinogen augmentation in chronic angiotensin II-infused mice. *Am J Physiol Renal Physiol*. 2008;295:F772-779. doi: 10.1152/ajprenal.00019.2008
40. Pucci G, Battista F, Anastasio F, Schillaci G. Morning pressor surge, blood pressure variability, and arterial stiffness in essential hypertension. *J Hypertens*. 2017;35:272-278. doi: 10.1097/HJH.0000000000001153
41. Wallace SM, Yasmin, McEniery CM, Maki-Petaja KM, Booth AD, Cockcroft JR, Wilkinson IB. Isolated systolic hypertension is characterized by increased aortic stiffness and endothelial dysfunction. *Hypertension*. 2007;50:228-233. doi: 10.1161/HYPERTENSIONAHA.107.089391
42. Sagie A, Larson MG, Levy D. The natural history of borderline isolated systolic hypertension. *N Engl J Med*. 1993;329:1912-1917. doi: 10.1056/NEJM199312233292602
43. Frishman WH. Cardiology patient page. Beta-adrenergic blockers. *Circulation*. 2003;107:e117-119. doi: 10.1161/01.CIR.0000070983.15903.A2
44. McAlister FA, Lethebe BC, Leung AA, Padwal RS, Williamson T. Visit-to-visit blood pressure variability is common in primary care patients: Retrospective cohort study of 221,803 adults. *PLoS One*. 2021;16:e0248362. doi: 10.1371/journal.pone.0248362
45. Suckow MA, Tirado-Muniz N. Seasonal Variation of Laboratory Animals as a Consideration for Research Reproducibility. *Comp Med*. 2023;73:255-259. doi: 10.30802/AALAS-CM-23-000033
46. Kastenmayer RJ, Fain MA, Perdue KA. A retrospective study of idiopathic ulcerative dermatitis in mice with a C57BL/6 background. *J Am Assoc Lab Anim Sci*. 2006;45:8-12.
47. Ogoh S, Tarumi T. Cerebral blood flow regulation and cognitive function: a role of arterial baroreflex function. *J Physiol Sci*. 2019;69:813-823. doi: 10.1007/s12576-019-00704-6
48. Teixeira SC, Madureira JB, Azevedo EI, Castro PM. Ageing affects the balance between central and peripheral mechanisms of cerebrovascular regulation with increasing influence of systolic blood pressure levels. *Eur J Appl Physiol*. 2019;119:519-529. doi: 10.1007/s00421-018-4036-3

748 49. Tarumi T, de Jong DL, Zhu DC, Tseng BY, Liu J, Hill C, Riley J, Womack KB, Kerwin DR, Lu H, et al.
749 Central artery stiffness, baroreflex sensitivity, and brain white matter neuronal fiber integrity in
750 older adults. *Neuroimage*. 2015;110:162-170. doi: 10.1016/j.neuroimage.2015.01.041
751 50. Brooks VL. Chronic infusion of angiotensin II resets baroreflex control of heart rate by an arterial
752 pressure-independent mechanism. *Hypertension*. 1995;26:420-424. doi:
753 10.1161/01.hyp.26.3.420
754 51. Hunyady L, Catt KJ, Clark AJ, Gaborik Z. Mechanisms and functions of AT(1) angiotensin receptor
755 internalization. *Regul Pept*. 2000;91:29-44. doi: 10.1016/s0167-0115(00)00137-3
756 52. Guo DF, Sun YL, Hamet P, Inagami T. The angiotensin II type 1 receptor and receptor-associated
757 proteins. *Cell Res*. 2001;11:165-180. doi: 10.1038/sj.cr.7290083
758 53. Zhang Y, Agnoletti D, Blacher J, Safar ME. Blood pressure variability in relation to autonomic
759 nervous system dysregulation: the X-CELLENT study. *Hypertens Res*. 2012;35:399-403. doi:
760 10.1038/hr.2011.203
761 54. Klein SP, De Sloovere V, Meyfroidt G, Depreitere B. Differential Hemodynamic Response of Pial
762 Arterioles Contributes to a Quadriphasic Cerebral Autoregulation Physiology. *J Am Heart Assoc*.
763 2022;11:e022943. doi: 10.1161/JAHA.121.022943
764 55. Fog M. The relationship between the blood pressure and the tonic regulation of the pial arteries.
765 *J Neurol Psychiatry*. 1938;1:187-197.
766 56. Lassen NA. Cerebral blood flow and oxygen consumption in man. *Physiol Rev*. 1959;39:183-238.
767 doi: 10.1152/physrev.1959.39.2.183
768 57. Kontos HA, Wei EP, Navari RM, Levasseur JE, Rosenblum WI, Patterson JL, Jr. Responses of
769 cerebral arteries and arterioles to acute hypotension and hypertension. *Am J Physiol*.
770 1978;234:H371-383.
771 58. Faraci FM, Mayhan WG, Heistad DD. Segmental vascular responses to acute hypertension in
772 cerebrum and brain stem. *Am J Physiol*. 1987;252:H738-742.
773 59. Faraci FM, Heistad DD. Regulation of large cerebral arteries and cerebral microvascular pressure.
774 *Circ Res*. 1990;66:8-17. doi: 10.1161/01.res.66.1.8
775 60. Iddings JA, Kim KJ, Zhou Y, Higashimori H, Filosa JA. Enhanced parenchymal arteriole tone and
776 astrocyte signaling protect neurovascular coupling mediated parenchymal arteriole vasodilation
777 in the spontaneously hypertensive rat. *J Cereb Blood Flow Metab*. 2015;35:1127-1136. doi:
778 10.1038/jcbfm.2015.31
779 61. Diaz JR, Kim KJ, Brands MW, Filosa JA. Augmented astrocyte microdomain Ca(2+) dynamics and
780 parenchymal arteriole tone in angiotensin II-infused hypertensive mice. *Glia*. 2019;67:551-565.
781 doi: 10.1002/glia.23564
782 62. Diaz-Otero JM, Fisher C, Downs K, Moss ME, Jaffe IZ, Jackson WF, Dorrance AM. Endothelial
783 Mineralocorticoid Receptor Mediates Parenchymal Arteriole and Posterior Cerebral Artery
784 Remodeling During Angiotensin II-Induced Hypertension. *Hypertension*. 2017;70:1113-1121. doi:
785 10.1161/HYPERTENSIONAHA.117.09598
786 63. Rigsby CS, Ergul A, Portik Dobos V, Pollock DM, Dorrance AM. Effects of spironolactone on cerebral
787 vessel structure in rats with sustained hypertension. *Am J Hypertens*. 2011;24:708-715. doi:
788 10.1038/ajh.2011.20
789 64. Koide M, Harraz OF, Dabertrand F, Longden TA, Ferris HR, Wellman GC, Hill-Eubanks DC,
790 Greenstein AS, Nelson MT. Differential restoration of functional hyperemia by antihypertensive
791 drug classes in hypertension-related cerebral small vessel disease. *J Clin Invest*. 2021;131. doi:
792 10.1172/JCI149029
793 65. Cipolla MJ, Sweet J, Chan SL, Tavares MJ, Gokina N, Brayden JE. Increased pressure-induced tone
794 in rat parenchymal arterioles vs. middle cerebral arteries: role of ion channels and calcium
795 sensitivity. *Journal of applied physiology*. 2014;117:53-59. doi: 10.1152/japplphysiol.00253.2014

796 66. Lozinskaya IM, Cox RH. Effects of age on Ca2+ currents in small mesenteric artery myocytes from
797 Wistar-Kyoto and spontaneously hypertensive rats. *Hypertension*. 1997;29:1329-1336. doi:
798 10.1161/01.hyp.29.6.1329
799 67. Simard JM, Li X, Tewari K. Increase in functional Ca2+ channels in cerebral smooth muscle with
800 renal hypertension. *Circulation research*. 1998;82:1330-1337. doi: 10.1161/01.res.82.12.1330
801 68. Pratt PF, Bonnet S, Ludwig LM, Bonnet P, Rusch NJ. Upregulation of L-type Ca2+ channels in
802 mesenteric and skeletal arteries of SHR. *Hypertension*. 2002;40:214-219. doi:
803 10.1161/01.hyp.0000025877.23309.36
804 69. Pesic A, Madden JA, Pesic M, Rusch NJ. High blood pressure upregulates arterial L-type Ca2+
805 channels: is membrane depolarization the signal? *Circulation research*. 2004;94:e97-104. doi:
806 10.1161/01.RES.0000131495.93500.3c
807 70. Sonkusare S, Palade PT, Marsh JD, Telemaque S, Pesic A, Rusch NJ. Vascular calcium channels and
808 high blood pressure: pathophysiology and therapeutic implications. *Vascul Pharmacol*.
809 2006;44:131-142. doi: 10.1016/j.vph.2005.10.005
810 71. Nieves-Cintron M, Syed AU, Nystoriak MA, Navedo MF. Regulation of voltage-gated potassium
811 channels in vascular smooth muscle during hypertension and metabolic disorders.
812 *Microcirculation*. 2018;25. doi: 10.1111/micc.12423
813 72. Navedo MF, Cheng EP, Yuan C, Votaw S, Molkentin JD, Scott JD, Santana LF. Increased coupled
814 gating of L-type Ca2+ channels during hypertension and Timothy syndrome. *Circulation research*.
815 2010;106:748-756. doi: 10.1161/CIRCRESAHA.109.213363
816 73. de la Sierra A. Blood Pressure Variability as a Risk Factor for Cardiovascular Disease: Which
817 Antihypertensive Agents Are More Effective? *J Clin Med*. 2023;12. doi: 10.3390/jcm12196167
818 74. Levi-Marpillat N, Macquin-Mavier I, Tropeano AI, Parati G, Maison P. Antihypertensive drug
819 classes have different effects on short-term blood pressure variability in essential hypertension.
820 *Hypertens Res*. 2014;37:585-590. doi: 10.1038/hr.2014.33
821 75. Kim KJ, Diaz JR, Presa JL, Muller PR, Brands MW, Khan MB, Hess DC, Althammer F, Stern JE, Filosa
822 JA. Decreased parenchymal arteriolar tone uncouples vessel-to-neuronal communication in a
823 mouse model of vascular cognitive impairment. *GeroScience*. 2021. doi: 10.1007/s11357-020-
824 00305-x
825 76. Chan SL, Nelson MT, Cipolla MJ. Transient receptor potential vanilloid-4 channels are involved in
826 diminished myogenic tone in brain parenchymal arterioles in response to chronic hypoperfusion
827 in mice. *Acta Physiol (Oxf)*. 2019;225:e13181. doi: 10.1111/apha.13181
828 77. Zhang D, Ma H, Liu C, Li Y. Relationship between morning blood pressure variability and cerebral
829 microbleed burden in patients with hypertension. *J Clin Hypertens (Greenwich)*. 2024;26:665-673.
830 doi: 10.1111/jch.14831
831 78. Ma Y, Yilmaz P, Bos D, Blacker D, Viswanathan A, Ikram MA, Hofman A, Vernooij MW, Ikram MK.
832 Blood Pressure Variation and Subclinical Brain Disease. *J Am Coll Cardiol*. 2020;75:2387-2399. doi:
833 10.1016/j.jacc.2020.03.043
834 79. Thorin-Trescases N, Bevan JA. High levels of myogenic tone antagonize the dilator response to
835 flow of small rabbit cerebral arteries. *Stroke; a journal of cerebral circulation*. 1998;29:1194-1200;
836 discussion 1200-1191. doi: 10.1161/01.str.29.6.1194
837 80. Tarantini S, Hertelendy P, Tucsek Z, Valcarcel-Ares MN, Smith N, Menyhart A, Farkas E, Hodges EL,
838 Towner R, Deak F, et al. Pharmacologically-induced neurovascular uncoupling is associated with
839 cognitive impairment in mice. *J Cereb Blood Flow Metab*. 2015;35:1871-1881. doi:
840 10.1038/jcbfm.2015.162
841 81. Ma J, Ayata C, Huang PL, Fishman MC, Moskowitz MA. Regional cerebral blood flow response to
842 vibrissal stimulation in mice lacking type I NOS gene expression. *Am J Physiol*. 1996;270:H1085-
843 1090. doi: 10.1152/ajpheart.1996.270.3.H1085

82. Lim XR, Abd-Alhaseeb MM, Ippolito M, Koide M, Senatore AJ, Plante C, Hariharan A, Weir N, Longden TA, Laprade KA, et al. Endothelial Piezo1 channel mediates mechano-feedback control of brain blood flow. *Nature communications*. 2024;15:8686. doi: 10.1038/s41467-024-52969-0
83. Tran CHT, Peringod G, Gordon GR. Astrocytes Integrate Behavioral State and Vascular Signals during Functional Hyperemia. *Neuron*. 2018;100:1133-1148 e1133. doi: 10.1016/j.neuron.2018.09.045
84. Renden RB, Institoris A, Sharma K, Tran CHT. Modulatory effects of noradrenergic and serotonergic signaling pathway on neurovascular coupling. *Commun Biol*. 2024;7:287. doi: 10.1038/s42003-024-05996-y
85. Epstein NU, Lane KA, Farlow MR, Risacher SL, Saykin AJ, Gao S. Cognitive dysfunction and greater visit-to-visit systolic blood pressure variability. *Journal of the American Geriatrics Society*. 2013;61:2168-2173. doi: 10.1111/jgs.12542
86. Sible IJ, Nation DA. Blood Pressure Variability and Cognitive Decline: A Post Hoc Analysis of the SPRINT MIND Trial. *Am J Hypertens*. 2023;36:168-175. doi: 10.1093/ajh/hpac128
87. Antunes M, Biala G. The novel object recognition memory: neurobiology, test procedure, and its modifications. *Cognitive processing*. 2012;13:93-110. doi: 10.1007/s10339-011-0430-z
88. Kraeuter AK, Guest PC, Sarnyai Z. The Y-Maze for Assessment of Spatial Working and Reference Memory in Mice. *Methods Mol Biol*. 2019;1916:105-111. doi: 10.1007/978-1-4939-8994-2_10
89. Liu N, Wang Y, An AY, Banker C, Qian YH, O'Donnell JM. Single housing-induced effects on cognitive impairment and depression-like behavior in male and female mice involve neuroplasticity-related signaling. *Eur J Neurosci*. 2020;52:2694-2704. doi: 10.1111/ejn.14565
90. Benfato ID, Quintanilha ACS, Henrique JS, Souza MA, Rosario BDA, Beserra Filho JIA, Santos RLO, Ribeiro AM, Le Sueur Maluf L, de Oliveira CAM. Effects of long-term social isolation on central, behavioural and metabolic parameters in middle-aged mice. *Behav Brain Res*. 2022;417:113630. doi: 10.1016/j.bbr.2021.113630
91. Magalhaes DM, Mampay M, Sebastiao AM, Sheridan GK, Valente CA. Age-related impact of social isolation in mice: Young vs middle-aged. *Neurochem Int*. 2024;174:105678. doi: 10.1016/j.neuint.2024.105678
92. Hu YY, Ding XS, Yang G, Liang XS, Feng L, Sun YY, Chen R, Ma QH. Analysis of the influences of social isolation on cognition and the therapeutic potential of deep brain stimulation in a mouse model. *Frontiers in psychiatry*. 2023;14:1186073. doi: 10.3389/fpsyt.2023.1186073
93. Panossian A, Cave MW, Patel BA, Brooks EL, Flint MS, Yeoman MS. Effects of age and social isolation on murine hippocampal biochemistry and behavior. *Mech Ageing Dev*. 2020;191:111337. doi: 10.1016/j.mad.2020.111337
94. Lander SS, Linder-Shacham D, Gaisler-Salomon I. Differential effects of social isolation in adolescent and adult mice on behavior and cortical gene expression. *Behav Brain Res*. 2017;316:245-254. doi: 10.1016/j.bbr.2016.09.005
95. Smolensky I, Zajac-Bakri K, Mallien AS, Gass P, Guzman R, Inta D. Effects of single housing on behavior, corticosterone level and body weight in male and female mice. *Lab Anim Res*. 2024;40:35. doi: 10.1186/s42826-024-00221-7

Figure 1. ***Experimental design and Ang II infusion effects on mean arterial pressure*.**
A, Schematic of the experimental design for middle-aged C57BL/6J male mice, including implantation of a chronic cranial window (-28 days from treatment onset) and an infusion pump with telemetry (-7 days from treatment onset). Infusion pumps were programmed for intermittent delivery of saline (baseline phase) or angiotensin II (Ang II) (treatment phase) at a rate of 18.4 μg/day, administered in 1-hour intervals every 3-4 hours. *In-vivo* two-photon (2P) imaging sessions were performed approximately 20 days into the treatment phase. Behavioral tests were conducted during the baseline period (Test 1) and 25 days into the treatment phase (Test 2). **B**, Representative raw traces depicting minute-to-minute, 24-hour MAP, SBP, DBP, PP, and Activity levels during intermittent saline infusions (left) and Ang II infusions (right). Dashed lines indicate periods of active infusion (1 hr) or when the pump is *on*. **C**, Average MAP, SBP, DBP, and PP (5 minutes) measured during infusion *Off* versus *On* conditions. **D**, 24-hour average MAP, SBP, DBP, and PP during a 5-day saline infusion phase (Baseline) and on Day 20 of Ang II treatment. Two-way ANOVA repeated measures followed by Sidak's multiple comparisons test (C, n = 8 BPV mice) (D, n = 13 control mice, n = 8 BPV mice).

Ang II=Angiotensin II, **BPV**=blood pressure variability, **DBP**=diastolic blood pressure **MAP**=mean arterial pressure, **PP**=pulse pressure, **SBP**=systolic blood pressure.

Figure 2. ***Effects of pulsatile BP on average 12:12 hour cardiovascular variables.***
A, Summary data of two-day averages of MAP, SBP (**B**), DBP (**C**), and PP (**D**) during the inactive (daylight) period (left column) and the active (nighttime) period (right column). Dashed rectangles indicate the baseline period (~5-day saline infusion). "*" and "&" denote within group comparisons ($p < 0.05$ vs Baseline) for BPV and control, respectively. "#" denotes $p<0.05$ between groups comparisons. Two-way ANOVA repeated measures followed by Sidak's comparison test; n = 13 control mice, n = 8 BPV mice.

BPV=blood pressure variability, **DBP**=diastolic blood pressure, **MAP**=mean arterial pressure, **PP**=pulse pressure, **SBP**=systolic blood pressure.

Table 1. ***Ang II-induced increases in blood pressure variability (BPV).***
A-B, Summary data of calculated two-day average real variability of MAP, SBP, DBP, and PP during the active period (**A**) and the inactive period (**B**). Baseline corresponds to (~5-day saline infusion) and "*" denotes within group comparisons ($p < 0.05$ vs Baseline) and "#" denotes $p < 0.05$ between groups comparisons. Two-way ANOVA repeated measures followed by Dunnett's comparison test; n = 13 control mice, n = 8 BPV mice.

ARV=average real variability, **BPV**=blood pressure variability, **DBP**=diastolic blood pressure, **MAP**= mean arterial pressure, **PP**=pulse pressure, **SBP**=systolic blood pressure.

Figure 3. ***Chronic BPV suppresses bradycardic reflex***.
A, Representative raw traces of 24-hour SBP (top) and HR (bottom) during intermittent Ang II infusions. **B**, Five-minute average HR when the infusion pump is *Off* or *On* (actively infusing Ang II) for control and BPV groups, extracted from the inactive (daytime) period. **C**, Twenty-four-hour average HR during the baseline period (~5-day saline infusion), and on day 20 of treatment (Day 20) for control and BPV mice. **D**,

933 Scatter plot of SBP and HR during Ang II infusion (100 minutes: 20 minutes before and after the 60-minute
934 pulse) in the inactive period for control and BPV mice (**E**). Linear trend lines for data shown in the insert.
935 Early and Late periods correspond to days 3-5 and days 23-25 of the treatment phase, respectively. **F,**
936 Scatter plot of SBP and HR during the active period in controls and in BPV mice (**G**). Two-way ANOVA
937 repeated measures followed by Sidak's multiple comparisons test (B-C, n = 6 control mice, n = 8 BPV mice).
938 Simple linear regression and "#" denotes $p < 0.05$ within group (D, F, n = 6 control mice) (E, G, n = 8 BPV
939 mice).
940
941 **bpm** = beats per minute, **BPV** = blood pressure variability, **HR** = heart rate, **SBP** = systolic blood pressure.
942
943 **Figure 4*. Norepinephrine infusion effects.***
944 **A,** Representative raw trace of minute-to-minute 24hr HR (top) and SBP (bottom). The green-shaded
945 region indicates the 1-hour period when the pump is actively infusing NE (45 µg/kg/min). **B,** Summary
946 data of two-day average MAP during the baseline phase (Dashed rectangle, ~5-day saline infusion) and
947 over 20 days of treatment. **C,** Summary data of calculated two-day ARV of SBP (left) and CV of SBP
948 (right). **D**, Scatter plot of SBP and HR during NE infusion (100-minute window: 20 minutes before and
949 after the 60-minute pulse) in the inactive (left) and active (right) periods, with linear trend lines shown in
950 the insert. Early and Late periods correspond to days 3-5 and days 16-20 of the treatment phase. "*"
951 and "#" denote within group comparisons ($p < 0.05$ vs Baseline) for Ang II- and NE-infused mice,
952 respectively. "&" and "Δ" denotes between group comparisons ($p<0.05$ vs control group) for Ang II- and
953 NE-infused mice, respectively. Two-way ANOVA repeated measures followed by Sidak's multiple
954 comparisons test (B-C, n = 6 mice). Simple linear regression (D, n = 3 mice).

955 **Ang II**=Angiotensin II, **bpm** = beats per minute, **HR** = heart rate, **NE** = norepinephrine, **SBP** = systolic blood
956 pressure.
957
958 **Figure 5. *Enhanced myogenic responses in parenchymal arterioles of BPV mice*.**
959 **A**, Schematic of the experimental set-up, including a portable telemetry system for continuous blood
960 pressure recordings alongside simultaneous 2P imaging of parenchymal arteriole diameter. **B**, Summary
961 data for the average imaging depth below the brain surface. **C**, Summary data for the average baseline
962 diameters of imaged parenchymal arterioles. **D**, Summary data of the average MAP recorded under
963 infusion pump *off* conditions (low blood pressure, Low BP) and infusion pump *on* conditions (high blood
964 pressure, High BP). **E**, Representative raw trace (from a single mouse) showing MAP (top) and
965 parenchymal arteriole diameter (bottom) over time. **F**, Expanded data corresponding to dashed region in
966 (**E**), highlighting Ang II-evoked BP changes. **G**, Representative scatter plot and linear regression of MAP vs
967 parenchymal arteriole diameter during an imaging session. **H**, Summary data of MAP-diameter linear
968 regression slopes. **I**, Relationship between minimum MAP recorded during an imaging run and the slope
969 shown in (**H**); dashed lines indicate the percent Δ change in MAP relative to its minimum value. The insert
970 provides a summary of percent Δ change in MAP from the minimum MAP. **J**, Scatter plot of MAP vs
971 changes in arteriole diameter from baseline pressure (~70 mmHg), spanning a pressure range 46-122
972 mmHg. Data subsets extracted from (**J**): (**K**) MAP ≤51 mmHg (orange dashed region), (**L**) MAP 51-100
973 mmHg (green dashed region), and (**M**) MAP ≥101 mmHg (blue dashed region). **N**, Illustration of the
974 proposed leftward shift (and narrower plateau) in cerebral autoregulatory curve induced by chronic BPV.
975 Unpaired t-test and Mann-Whitney test (B-C, H-I, n = 10 runs/8 control mice, n = 11 runs/8 BPV mice).
976 Two-way ANOVA repeated measures followed by Sidak's multiple comparison test (D, n = 10 runs/8

control mice, n = 11 runs/8 BPV mice). Simple linear regression and "#" denotes $p < 0.05$ between group (J-M, n = 12 runs/9 control mice, n = 8 runs/7 BPV mice).

BPV = blood pressure variability, **MAP** = mean arterial pressure

Figure 6. ***Suppressed neurovascular responses in parenchymal arterioles of BPV during low and high blood pressure periods.***

A, Schematic of the experimental setup in which a picospritzer delivered a puff of air for whisker stimulation (WS) at 10 Hz for 20 seconds. **B**, Representative image showing the mask (outlined) used to track changes in parenchymal arteriole diameter. **C**, Summarized data of average MAP recorded during low blood pressure (Low BP; pump *off*) and high blood pressure (High BP; pump *on*) conditions. **D**, Summary data of the average imaging depth below the brain surface. **E**, Representative raw trace (from a single mouse) showing MAP (top) and parenchymal arteriole diameter (bottom) during low and high blood pressure. Dashed green squares indicate WS response, with "a" denoting the 30-second pre-stimulus diameter and "b" denoting the 30-second post-stimulus diameter, summarized in (**F**). **G**, Normalized averaged arteriole diameter traces with corresponding error bars (dashed lines) during the WS response, shown as % change from baseline (20 seconds before stimulus), during the 20-second stimulus (green shaded region), and 64 seconds post-stimulus (green dashed square). **H,** Summarized data of stimulus-induced arteriole responses (green shaded region in **G**). **I**, Summary data of recovery time, with rate of decay (k) corresponding to 30-second post-stimulus period outlined in the green dashed square in (**G**). Two-way ANOVA repeated measures followed by Sidak's multiple comparisons test (C-D, n = 7 control mice, 5 BPV mice) (F, n = 5-8 control mice, n = 6-7 BPV mice) and (H, n = 5-8 control mice, n = 6-7 BPV mice). One phase exponential decay nonlinear fit (I, n = 5-8 control mice, n = 6-7 BPV mice).

BPV = blood pressure variability, ***k*** = rate of decay, **MAP** = mean arterial pressure, **WS** = whisker stimulation

Figure 7. ***Behavior and altered cognitive function of BPV mice*.**

A, Schematic of the novel object recognition test with a 1-hour delay between the A-A and A-B trials (top), accompanied by summarized recognition and discriminatory index data for mice during the saline infusion period (baseline) and following 25 days of pulsatile Ang II infusion (Ang II). **B**, Diagram of 10-minute spontaneous Y-maze experimental setup (top) and the summary of % alternation and distance traveled during baseline and after 25 days of Ang II treatment (bottom). **C,** Summary data of two-day, 24-hour activity averages throughout treatment during active and inactive periods, with the Baseline phase (~5-day saline infusion) marked by the dashed rectangle. **D,** Summary data of 24-hour averaged activity recorded when the infusion pump was *on* vs *off* during Early (days 3-5) and Late (days 23-25) treatment phases. (**E**) Summary of activity when the pump is *on* vs *off* during the Early and Late phases of treatment for the inactive cycle. (**F**) Summary of activity when the pump is *on* vs *off* during the Early and Late phases of treatment for the active cycle. Paired t-test (A, n = 10 BPV mice), (B, n = 11 BPV mice). Two-way ANOVA repeated measures followed by Tukey's comparison test (C, n = 13 control mice, n = 8 BPV mice) (D-F, n = 6 control mice, n = 8 BPV mice). "*" denotes $p < 0.05$ vs Baseline for control, active period. "$" and "Δ" denote $p<0.05$ (active vs inactive period) for control and BPV, respectively.

AU=arbitrary units, **BPV**=blood pressure variability

1021
1022 **Supplemental Table 1.** ***Pulsatile Ang II infusions induced an increase in blood pressure variability (BPV)***
1023 ***measured by coefficient of variance.***
1024 **A-B**, Summary data of calculated two-day average coefficient of variance (CV) of MAP, SBP, DBP, and PP
1025 during the active period (**A**) and inactive period (**B**). CV was calculated as the ratio of the standard
1026 deviation of hourly BP averages to 24-hour mean blood pressure. Two-way ANOVA repeated measures
1027 followed by Dunnett's comparison test; n = 13 control mice, n = 8 BPV mice. "*" denotes $p < 0.05$ vs
1028 Baseline and "#" denotes $p < 0.05$ between groups.
1029
1030 **BPV** = blood pressure variability, **CV**, coefficient of variance, **DBP** = diastolic blood pressure, **MAP** = mean
1031 arterial pressure, **PP** = pulse pressure, **SBP** = systolic blood pressure.
1032
1033 **Supplemental Figure 1***. Exclusion criteria for myogenic response analysis.*
1034 **A-B**, Representative raw traces (from one mouse) of MAP (top) and parenchymal arteriole diameter
1035 (bottom) showing WS-evoked dilations (**A**) and random dilatory events (**B**). Grey dashed rectangles outline
1036 the period when the pump is on and BP transitions to higher values (Ang II infusion). **C-D**, Expanded data
1037 corresponding to the dashed rectangle shown in (**A-B**), with dilatory responses to WS outlined within
1038 green dashed rectangles (**C**) and transient dilatory events shown within orange dashed rectangles (**D**). **E-**
1039 **F**, Representative raw traces of MAP (top) and parenchymal arteriole diameter (bottom) following
1040 removal of sensory-evoked dilations (**C**) or the random dilatory events outlined in (**D**). **G-H**, Scatter plot
1041 and resultant linear regression line of the filtered MAP vs parenchymal diameter corresponding to (**E-F**).
1042
1043 **MAP** = mean arterial pressure
1044
1045 **Supplemental Figure 2***. Seasonal effects on mean arterial pressure.*
1046 **A,** Summarized data of 24-hr MAP at baseline (5 days saline infusion) in mice with (+) or without (-) a
1047 cranial window. **B**, Summarized data of two-day average MAP at baseline and 20 days of treatment.
1048 Spring-Summer corresponds to warmer months (May-September), and Fall-Winter corresponds to colder
1049 months (October-April). Mann-Whitney test (A, n = 14 mice with craniotomy, 6 without craniotomy). Two-
1050 way ANOVA repeated measures followed by Sidak's multiple comparisons test (B, n = 11 mice in Spring-
1051 Summer, 9 mice in Fall-Winter).
1052
1053 **MAP** = mean arterial pressure
1054
1055 **Supplemental Figure 3***. One-hour averages of MAP over 24hrs-Circadian Profile*
1056 **A,** Representative raw trace of one-hour average MAP for 24hrs of all control mice and BPV mice (**B**), with
1057 controls summarized in (**C**) and BPV in (**D**). *Inactive* corresponds to daylight hours (6am-6pm). (A-D, n = 13
1058 control mice, n = 8 BPV mice).
1059
1060 **BPV**=blood pressure variability, **MAP** = mean arterial pressure
1061
1062 **Supplemental Figure 4***. Transient Ang II infusions induced pulsatile blood pressure in control mice.*

1063 Summary data of averaged BP (5 minutes) while the pump is *Off* or *On* and infusing Ang II in controls. Data
1064 was extracted from the inactive (daytime) period at days 3-5 of treatment protocol. Paired Wilcoxon test
1065 (n = 6 control mice).
1066
1067 **DBP** = diastolic blood pressure, **MAP** = mean arterial pressure, **PP** = pulse pressure, **SBP** = systolic blood
1068 pressure.
1069
1070 **Supplemental Figure 5*. Directional myogenic responses***
1071 **A,** Summary data for averaged BP corresponding to the Low-to-High BP transition. **B,** Representative raw
1072 trace showing MAP (top) and parenchymal arteriole diameter (bottom) during Low-to-High MAP
1073 transition shaded in orange (left) and the corresponding representative scatter plot of MAP vs
1074 parenchymal arteriole diameter (right). **C,** Summary of MAP-diameter linear regression slopes
1075 corresponding to Low-to-High MAP transition. **D,** Summary data of the average high and low MAP
1076 recorded immediately following cessation of pump infusion and blood pressure transitions from high to
1077 low BP (High-to-Low). **E,** Representative raw trace showing MAP (top) and parenchymal arteriole diameter
1078 (bottom) during High-to-Low MAP transition shaded in green (left) and the corresponding representative
1079 scatter plot of MAP vs parenchymal arteriole diameter (right). **F,** Summary of MAP-diameter linear
1080 regression slopes corresponding to High-to-Low MAP transition. Two-way ANOVA repeated measures
1081 followed by Sidak's multiple comparisons test (A, n = 12 runs/7 control mice, n = 14 runs/8 BPV mice) (D,
1082 n = 10 runs/8 control mice, n = 12 runs/7 BPV mice). Unpaired t-test and Mann-Whitney test (C, n = 12
1083 runs/7 control mice, n = 14 runs/8 BPV mice) (F, n = 10 runs/8 control mice, n = 12 runs/7 BPV mice).
1084
1085 **BPV**=blood pressure variability, **MAP** = mean arterial pressure
1086
1087

Figure 1

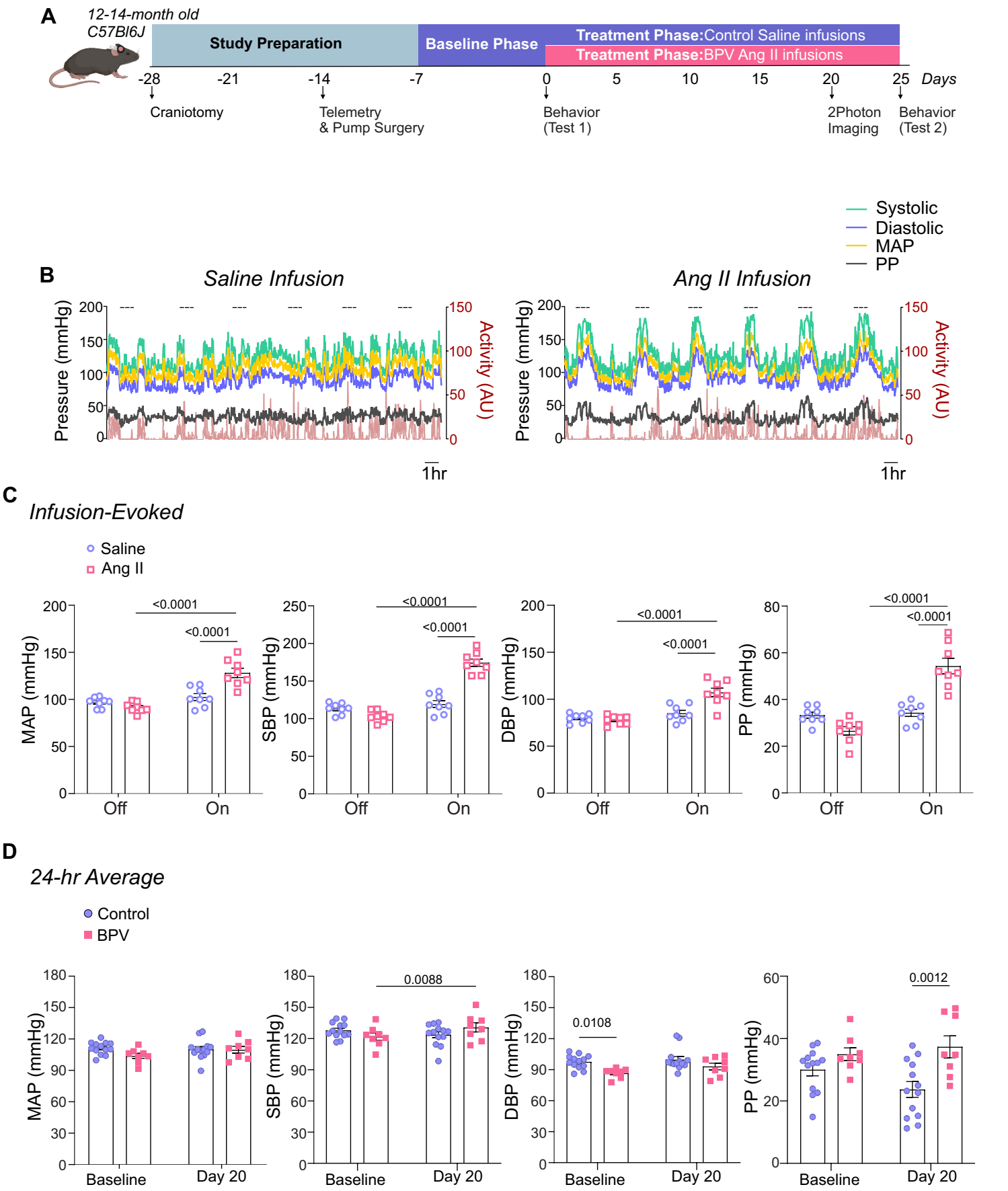
A
12-14-month old
C57Bl6J
Study Preparation
Baseline Phase
Treatment Phase:Control Saline infusions
Treatment Phase:BPV Ang II infusions
-28
-21
-14
-7
0
5
10
15
20
25
Days
Craniotomy
Telemetry
& Pump Surgery
Behavior
(Test 1)
2Photon
Imaging
Behavior
(Test 2)
Systolic
Diastolic
MAP
PP
B
Saline Infusion
Ang II Infusion
Pressure (mmHg)
Activity (AU)
1hr
C
Infusion-Evoked
Saline
Ang II
MAP (mmHg)
SBP (mmHg)
DBP (mmHg)
PP (mmHg)
<0.0001
Off
On
D
24-hr Average
Control
BPV
0.0088
0.0108
0.0012
Baseline
Day 20

Figure 2

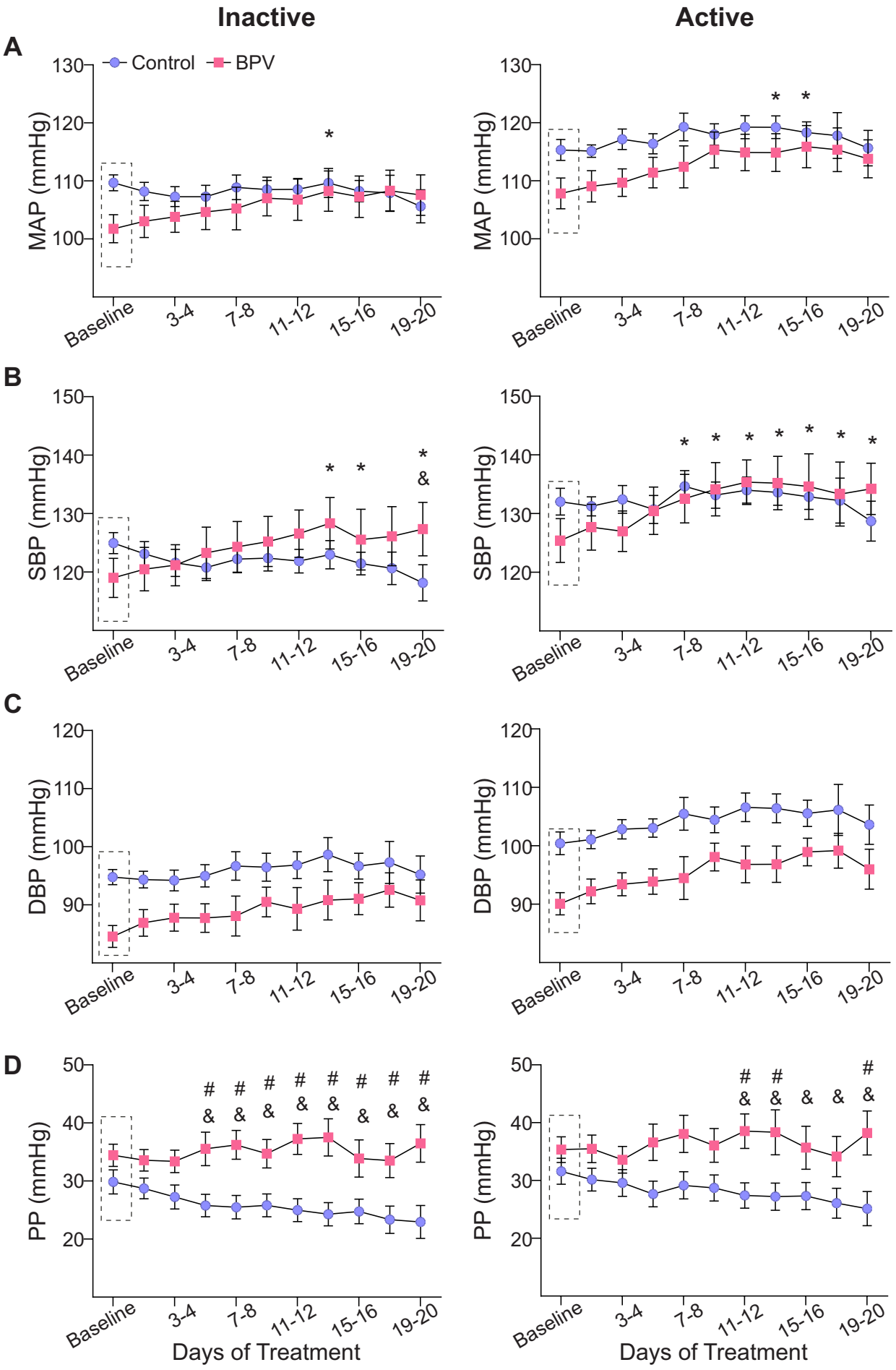
Inactive
Active
A
Control
BPV
MAP (mmHg)
B
SBP (mmHg)
C
DBP (mmHg)
D
PP (mmHg)
Baseline
3-4
7-8
11-12
15-16
19-20
Days of Treatment

Figure 3

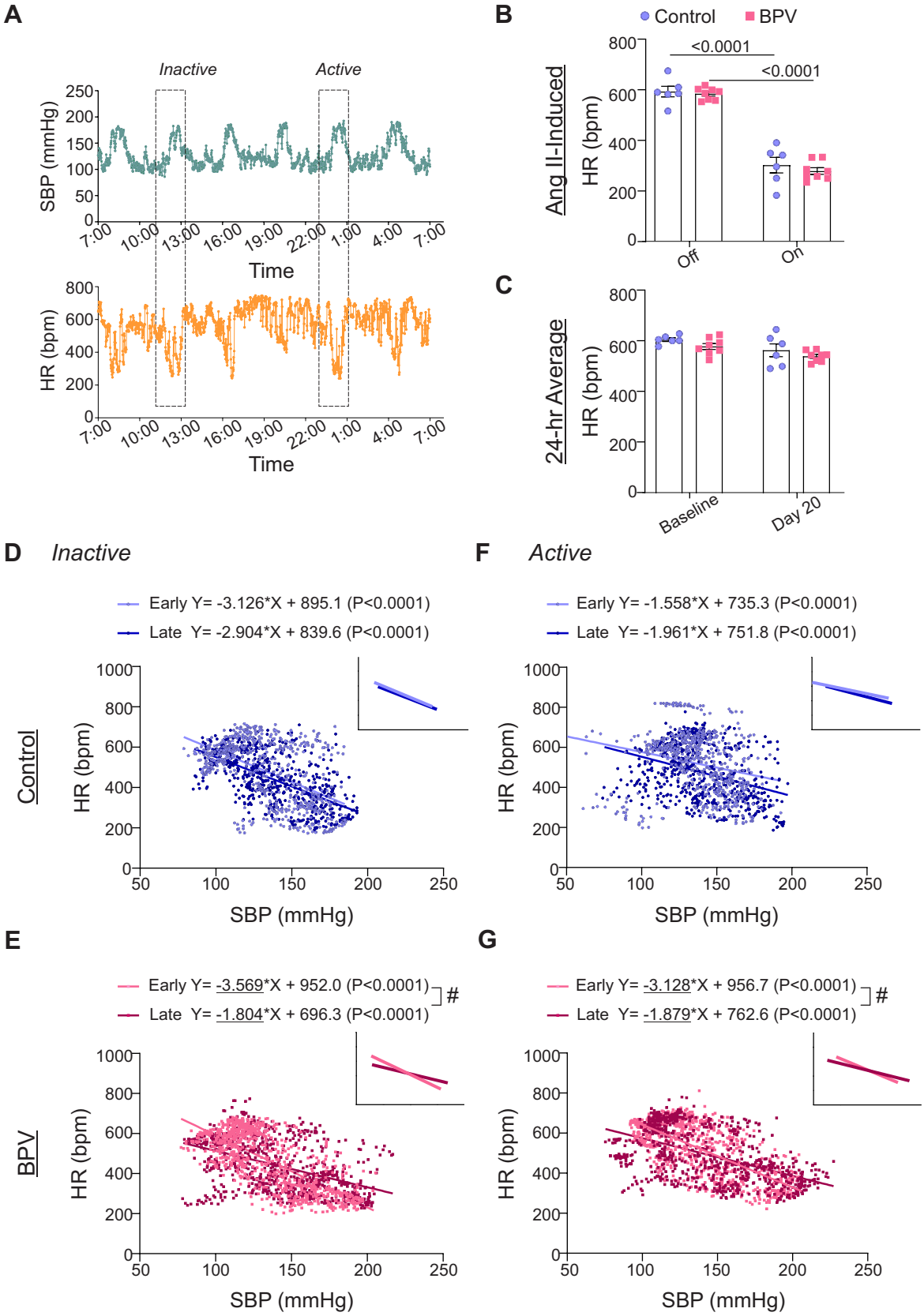
A
Inactive
Active
SBP (mmHg)
HR (bpm)
Time
B
Control
BPV
Ang II-Induced
HR (bpm)
<0.0001
<0.0001
Off
On
C
24-hr Average
HR (bpm)
Baseline
Day 20
D
Inactive
Early Y= -3.126*X + 895.1 (P<0.0001)
Late Y= -2.904*X + 839.6 (P<0.0001)
Control
HR (bpm)
SBP (mmHg)
F
Active
Early Y= -1.558*X + 735.3 (P<0.0001)
Late Y= -1.961*X + 751.8 (P<0.0001)
HR (bpm)
SBP (mmHg)
E
Early Y= -3.569*X + 952.0 (P<0.0001)
Late Y= -1.804*X + 696.3 (P<0.0001)
#
BPV
HR (bpm)
SBP (mmHg)
G
Early Y= -3.128*X + 956.7 (P<0.0001)
Late Y= -1.879*X + 762.6 (P<0.0001)
#
HR (bpm)
SBP (mmHg)

Figure 4

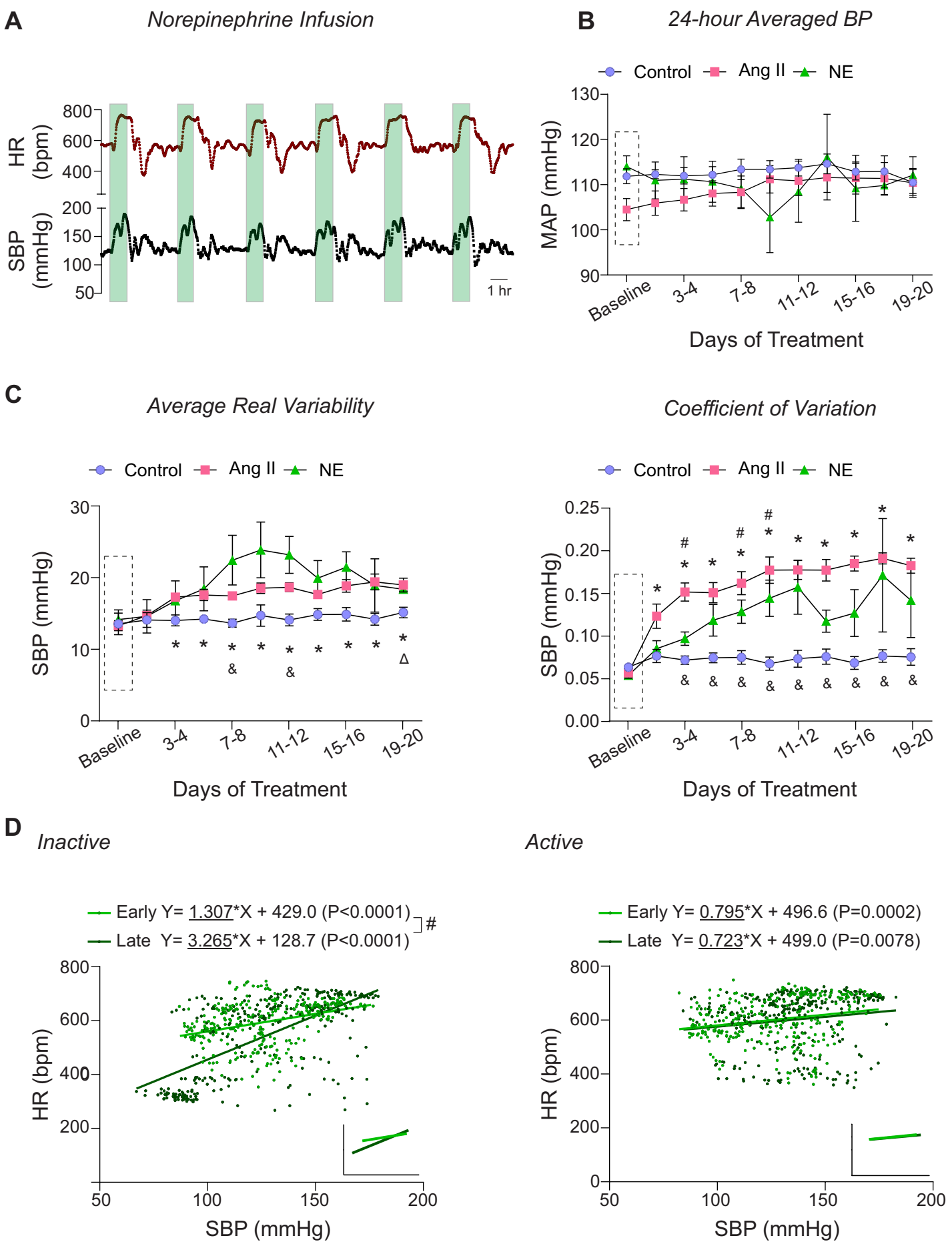
A
Norepinephrine Infusion
HR (bpm)
800
600
400
SBP (mmHg)
200
150
100
50
1 hr
B
24-hour Averaged BP
Control
Ang II
NE
MAP (mmHg)
130
120
110
100
90
Baseline
3-4
7-8
11-12
15-16
19-20
Days of Treatment
C
Average Real Variability
Control
Ang II
NE
SBP (mmHg)
30
20
10
0
Baseline
3-4
7-8
11-12
15-16
19-20
Days of Treatment
Coefficient of Variation
Control
Ang II
NE
SBP (mmHg)
0.25
0.20
0.15
0.10
0.05
0.00
Baseline
3-4
7-8
11-12
15-16
19-20
Days of Treatment
D
Inactive
Early Y= 1.307*X + 429.0 (P<0.0001)
Late Y= 3.265*X + 128.7 (P<0.0001)
#
HR (bpm)
800
600
400
200
50
100
150
200
SBP (mmHg)
Active
Early Y= 0.795*X + 496.6 (P=0.0002)
Late Y= 0.723*X + 499.0 (P=0.0078)
HR (bpm)
800
600
400
200
0
50
100
150
200
SBP (mmHg)

Figure 5

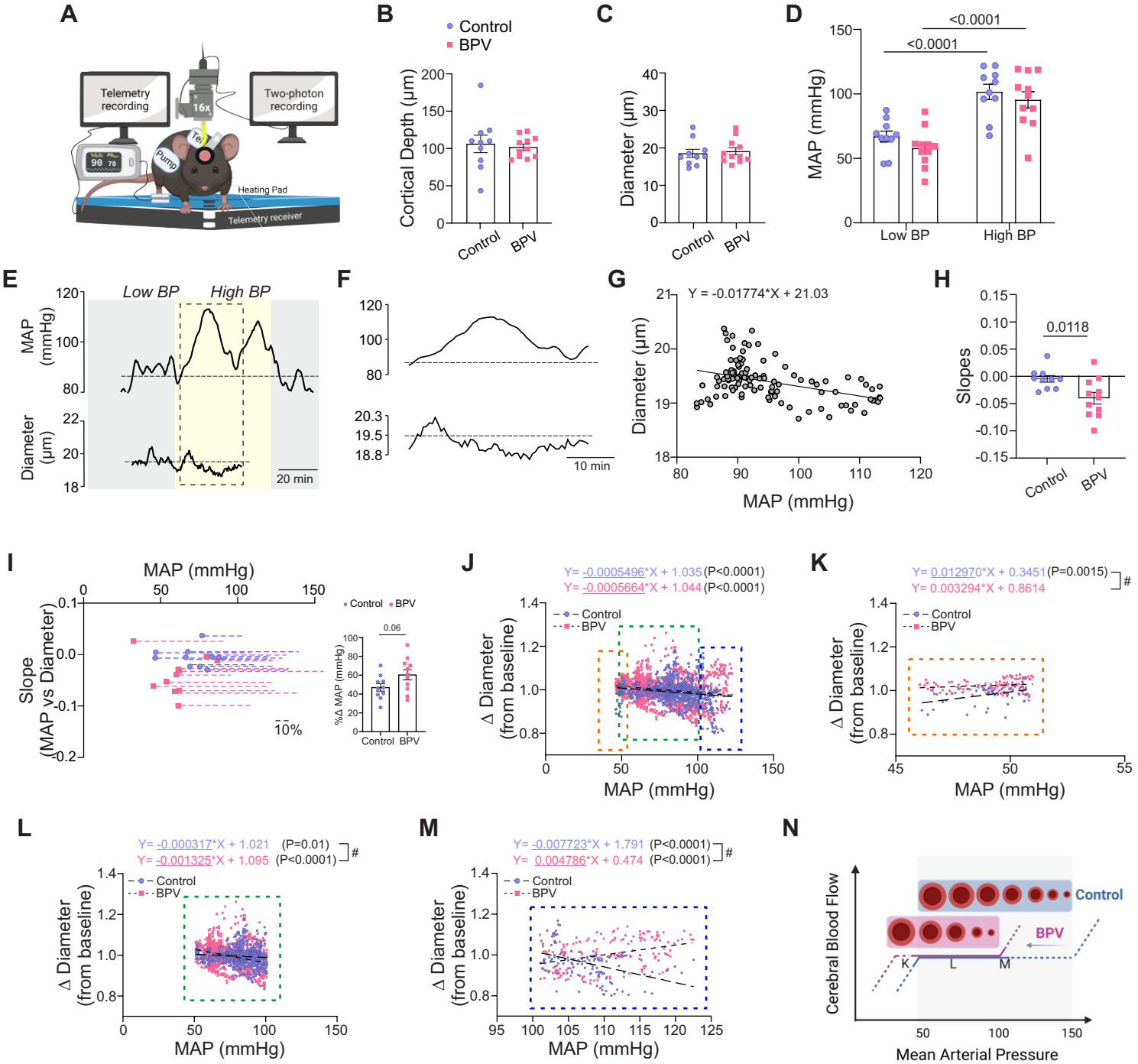
A
Telemetry recording
Two-photon recording
16x
Pump
Heating Pad
Telemetry receiver
B
Control
BPV
Cortical Depth (µm)
Control
BPV
C
Diameter (µm)
Control
BPV
D
<0.0001
<0.0001
MAP (mmHg)
Low BP
High BP
E
Low BP
High BP
MAP (mmHg)
Diameter (µm)
20 min
F
10 min
G
Y = -0.01774*X + 21.03
Diameter (µm)
MAP (mmHg)
H
0.0118
Slopes
Control
BPV
I
MAP (mmHg)
Slope (MAP vs Diameter)
10%
Control
BPV
0.06
%Δ MAP (mmHg)
Control
BPV
J
Y= -0.0005496*X + 1.035 (P<0.0001)
Y= -0.0005664*X + 1.044 (P<0.0001)
Control
BPV
Δ Diameter (from baseline)
MAP (mmHg)
K
Y= 0.012970*X + 0.3451 (P=0.0015)
Y= 0.003294*X + 0.8614
#
Control
BPV
Δ Diameter (from baseline)
MAP (mmHg)
L
Y= -0.000317*X + 1.021 (P=0.01)
Y= -0.001325*X + 1.095 (P<0.0001)
#
Control
BPV
Δ Diameter (from baseline)
MAP (mmHg)
M
Y= -0.007723*X + 1.791 (P<0.0001)
Y= 0.004786*X + 0.474 (P<0.0001)
#
Control
BPV
Δ Diameter (from baseline)
MAP (mmHg)
N
Control
BPV
K
L
M
Cerebral Blood Flow
Mean Arterial Pressure

Figure 6

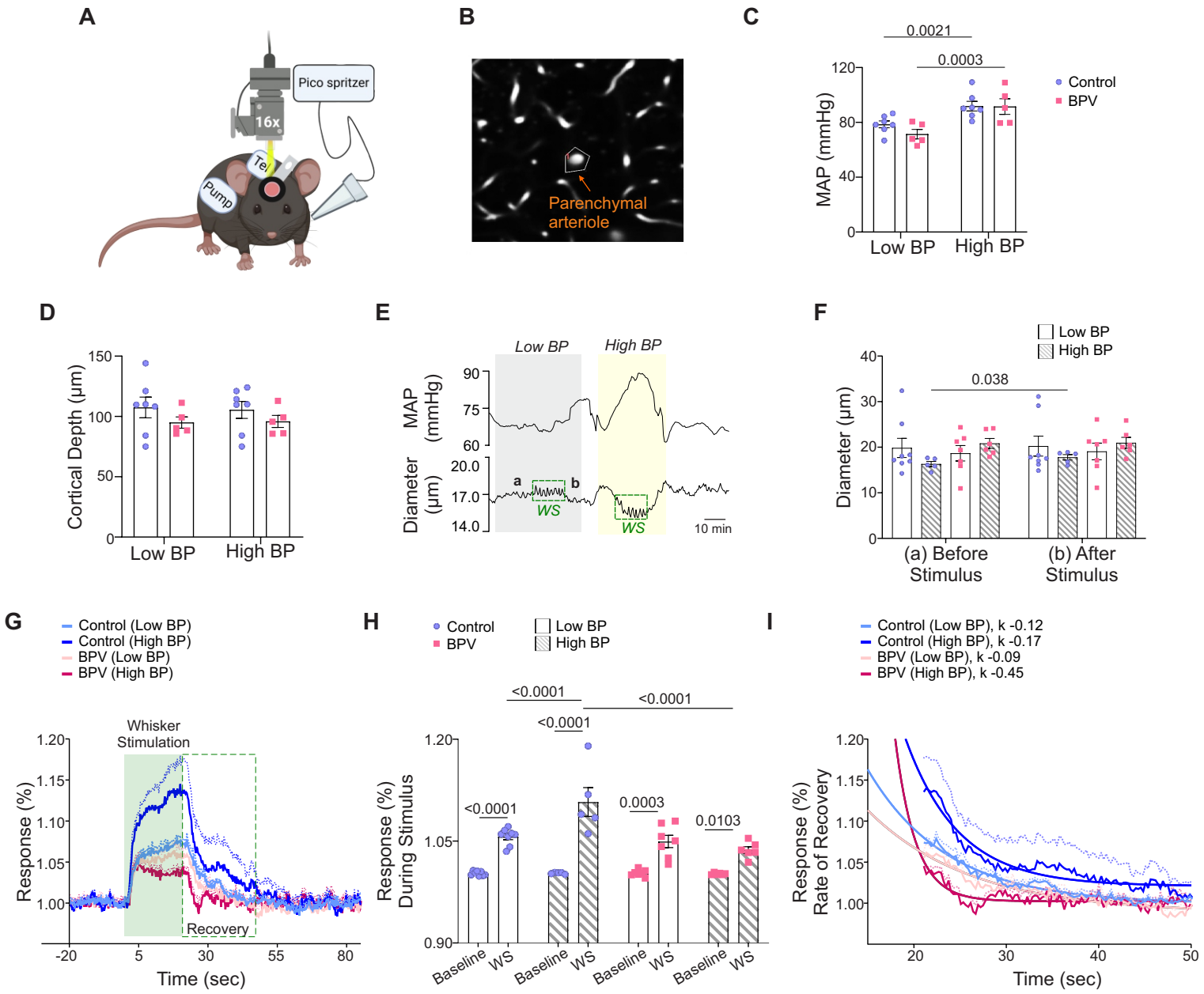
A
Pico spritzer
16x
Pump
B
Parenchymal arteriole
C
0.0021
0.0003
MAP (mmHg)
Control
BPV
Low BP
High BP
D
Cortical Depth (µm)
Low BP
High BP
E
Low BP
High BP
MAP (mmHg)
Diameter (µm)
a
b
WS
WS
10 min
F
Low BP
High BP
0.038
Diameter (µm)
(a) Before Stimulus
(b) After Stimulus
G
Control (Low BP)
Control (High BP)
BPV (Low BP)
BPV (High BP)
Whisker Stimulation
Recovery
Response (%)
Time (sec)
H
Control
BPV
Low BP
High BP
<0.0001
<0.0001
<0.0001
<0.0001
0.0003
0.0103
Response (%) During Stimulus
Baseline
WS
I
Control (Low BP), k -0.12
Control (High BP), k -0.17
BPV (Low BP), k -0.09
BPV (High BP), k -0.45
Response (%) Rate of Recovery
Time (sec)

Figure 7

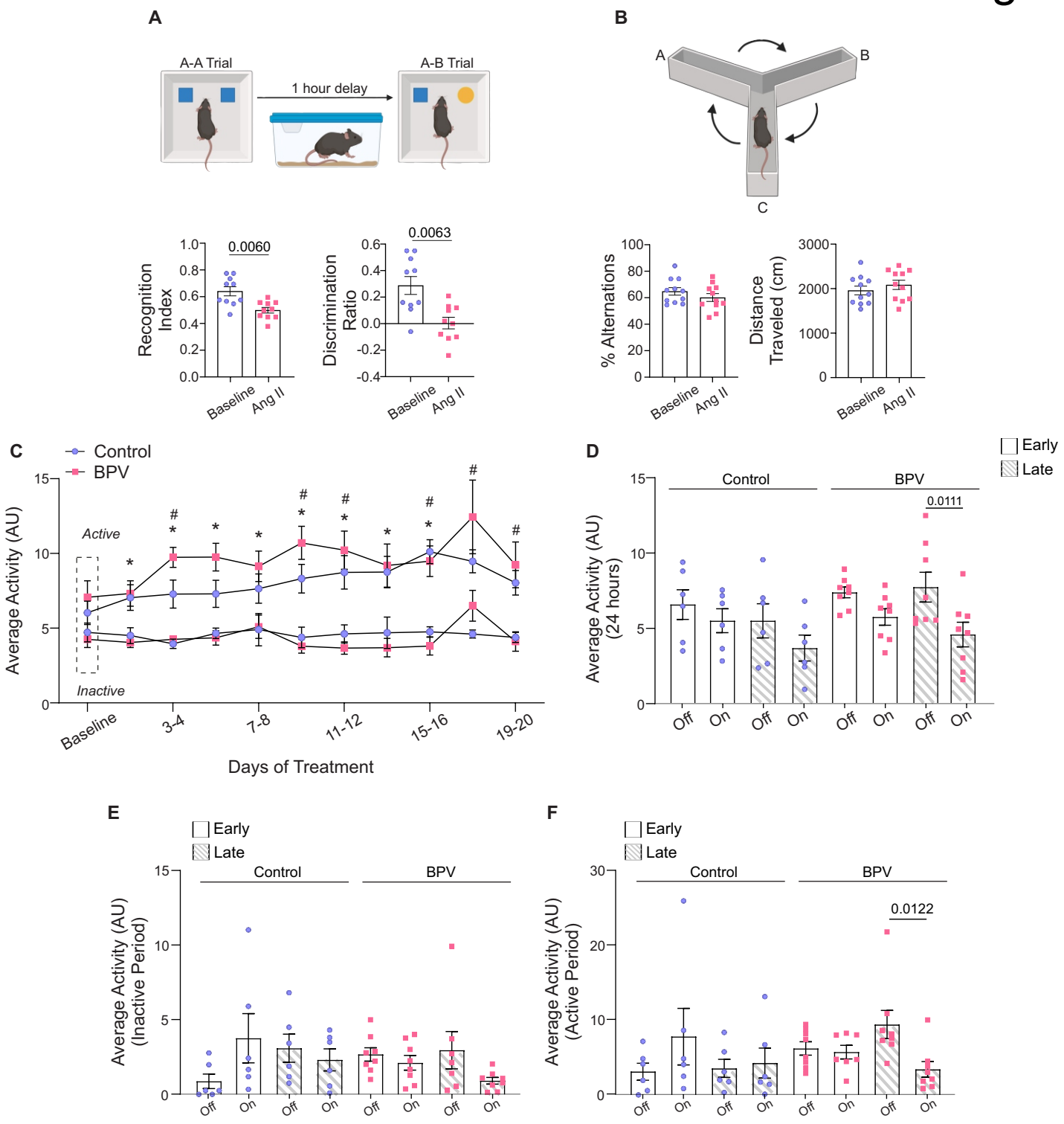
A
A-A Trial
1 hour delay
A-B Trial
B
A
B
C
Recognition Index
0.0060
Baseline
Ang II
Discrimination Ratio
0.0063
% Alternations
Distance Traveled (cm)
C
Control
BPV
Active
Inactive
Average Activity (AU)
Baseline
3-4
7-8
11-12
15-16
19-20
Days of Treatment
D
Early
Late
Control
BPV
0.0111
Average Activity (AU) (24 hours)
Off
On
E
Average Activity (AU) (Inactive Period)
F
Average Activity (AU) (Active Period)
0.0122

Table 1

A

Active Period ARV mmHg ± SEM

Days	MAP		SBP		DBP		PP	
	Control	BPV	Control	BPV	Control	BPV	Control	BPV
Baseline	*12.44 ± 1.37*	*10.94 ± 0.55*	*14.15 ± 1.49*	*13.13 ± 0.66*	*11.53 ± 1.44*	*9.04 ± 0.54*	*4.67 ± 0.40*	*5.47 ± 0.46*
1-2	12.91 ± 1.29	10.99 ± 0.35	14.86 ± 1.28	14.56 ± 0.44	11.70 ± 1.48	9.29 ± 0.41	5.12 ± 0.40	7.67 ± 0.69
3-4	12.44 ± 0.66	12.51 ± 0.43	14.40 ± 0.67	16.40 ± 0.66 *	11.12 ± 0.83	10.35 ± 0.45	5.03 ± 0.33	8.12 ± 0.71 *#
5-6	11.78 ± 0.52	12.80 ± 0.39	13.64 ± 0.61	16.44 ± 0.53 *#	10.71 ± 0.73	10.54 ± 0.45	4.89 ± 0.32	7.99 ± 0.69 *#
7-8	12.35 ± 0.61	12.85 ± 0.41 *	14.02 ± 0.67	16.73 ± 0.43 *#	11.37 ± 0.81	10.61 ± 0.55 *	5.22 ± 0.42	8.34 ± 0.74 *#
9-10	12.34 ± 0.69	12.84 ± 0.40	13.88 ± 0.75	16.37 ± 0.72	11.32 ± 0.79	10.82 ± 0.24	4.95 ± 0.39	7.86 ± 0.65 *#
11-12	13.00 ± 0.76	12.94 ± 0.76 *	14.59 ± 0.88	16.87 ± 0.70 *	11.93 ± 0.93	10.59 ± 0.81	5.05 ± 0.34	8.25 ± 0.78 #
13-14	12.26 ± 0.84	12.90 ± 0.42 *	13.94 ± 0.84	16.80 ± 0.52 *	11.17 ± 0.95	10.40 ± 0.68 *	5.07 ± 0.39	8.45 ± 0.83 #
15-16	13.27 ± 0.59	13.91 ± 1.02	15.11 ± 0.81	17.50 ± 0.87 *	11.72 ± 0.82	11.59 ± 1.14	5.24 ± 0.38	8.25 ± 0.73 *
17-18	13.12 ± 0.77	14.06 ± 0.92	15.16 ± 1.03	17.12 ± 0.77 *	11.99 ± 0.85	11.95 ± 1.19	5.48 ± 0.58	7.60 ± 0.77
19-20	12.62 ± 0.45	12.75 ± 0.92	14.75 ± 0.52	16.57 ± 0.94	11.09 ± 0.70	10.48 ± 1.23	6.32 ± 0.60	8.44 ± 1.15

B

Inactive Period ARV mmHg ± SEM

Days	MAP		SBP		DBP		PP	
	Control	BPV	Control	BPV	Control	BPV	Control	BPV
Baseline	*12.09 ± 1.38*	*11.29 ± 0.54*	*13.53 ± 1.50*	*13.28 ± 0.70*	*11.27 ± 1.40*	*9.48 ± 0.45*	*4.74 ± 0.47*	*5.04 ± 0.45*
1-2	12.15 ± 1.04	11.40 ± 0.69	14.08 ± 1.03	14.69 ± 0.77	10.95 ± 1.15	9.76 ± 0.68	4.92 ± 0.24	7.09 ± 0.55
3-4	12.23 ± 0.79	13.38 ± 0.33 *	14.02 ± 0.76	17.27 ± 0.48 *#	11.19 ± 1.02	11.29 ± 0.47 *	4.76 ± 0.32	7.90 ± 0.55 *#
5-6	12.16 ± 0.43	13.63 ± 0.78 *	13.64 ± 0.52	17.57 ± 0.78 *#	10.68 ± 0.53	11.34 ± 0.86	4.95 ± 0.30	8.23 ± 0.69 *#
7-8	11.95 ± 0.49	13.73 ± 0.50 *	14.71 ± 0.54	17.44 ± 0.53 *#	10.88 ± 0.59	11.61 ± 0.67 *	4.90 ± 0.32	8.45 ± 0.89
9-10	12.90 ± 1.28	14.77 ± 0.66 *	14.09 ± 1.49	18.52 ± 0.72 *	11.92 ± 1.15	12.59 ± 0.64 *	5.33 ± 0.31	8.16 ± 0.61 *#
11-12	12.49 ± 0.79	14.53 ± 0.57 *	14.85 ± 0.82	18.65 ± 0.62 *#	11.50 ± 1.07	12.09 ± 0.74 *	5.24 ± 0.31	8.50 ± 0.88
13-14	13.03 ± 0.75	13.96 ± 0.74 *	14.85 ± 0.82	17.65 ± 0.53 *	11.94 ± 0.99	11.56 ± 0.92	5.10 ± 0.38	8.16 ± 0.74 *#
15-16	13.35 ± 0.79	15.04 ± 0.87 *	14.87 ± 0.93	18.85 ± 0.87 *	12.21 ± 0.98	12.66 ± 1.07	4.97 ± 0.36	8.54 ± 1.06 *
17-18	12.99 ± 0.70	15.61 ± 1.36	14.19 ± 0.82	19.39 ± 1.09 *#	11.47 ± 0.83	13.18 ± 1.67	5.02 ± 0.40	8.46 ± 1.03
19-20	12.89 ± 0.57	14.72 ± 1.00 *	15.13 ± 0.74	18.96 ± 0.96 *	11.36 ± 0.65	12.19 ± 1.25	6.21 ± 0.40	9.28 ± 1.33